

Harmful Algal Blooms in Select New Jersey Coastal Lakes

2021-2023

Authors and Affiliation:

Jason E. Adolf, Ph.D.

Monmouth University

Prepared for:

New Jersey Department of Environmental Protection

Division of Science and Research

Project Manager: Rob Newby, Ph.D.

June 4th, 2025

Funded by the New Jersey Department of Environmental Protection through an agreement with EPA under Contract Numbers SR21-007 & SR23-010.

State of New Jersey
Phil Murphy, Governor

Department of Environmental Protection
Shawn M. LaTourette, Commissioner



Division of Science & Research
Nicholas A. Procopio, Ph.D., Director

Visit the DSR website:
<https://dep.nj.gov/dsr>

Acknowledgements:

Erin Conlon – Community science coordinator and primary laboratory / field technician

Ariel Zavala – Monmouth University undergraduate student, 2021

Marie Mauro – Monmouth University undergraduate student, summer 2022

Chris Riegel – Monmouth University undergraduate student, summer 2023

Griffin Adolf – Monmouth University undergraduate student, summers 2022 & 2023

Nicholas Occhiogrosso – Monmouth University undergraduate student, summer 2022

Diederik Boonman-Morales – Monmouth University undergraduate student, 2022, 2023, 2024

Emma Najarian – Rumson-Fairhaven High School student volunteer, 2023

Dylan DiBella -- Monmouth University undergraduate student, 2024-2025

Thank you to the NJDEP Leeds Point laboratory (Eric Ernst, Dawn Thompson, and their talented staff) for providing nutrient analyses of coastal lakes samples.

Please cite as: Adolf, J. E. 2025. Harmful Algal Blooms in Select New Jersey Coastal Lakes. New Jersey Department of Environmental Protection. Trenton, NJ. 37 pages. Available at <https://hdl.handle.net/10929/149296>.

Table of Contents

Executive Summary	4
Project objectives / hypotheses / summary results.....	4
Introduction	6
Methodology and QAPP	7
<i>Study Area</i>	7
<i>Field Measurements and sample collections</i>	10
<i>Algal Analysis</i>	11
<i>Quantitative gene analysis (qPCR) for 16s and toxin genes in cyanobacteria</i>	11
<i>eDNA sample collection and processing</i>	12
Water Collection.....	12
Filtration and Processing.....	12
Molecular analysis.....	12
Bioinformatics and biodiversity analyses.....	12
Data Inventory.....	13
Results	14
<i>Summary for hypothesis #1</i>	19
<i>Summary for hypothesis #2</i>	22
<i>Summary for hypothesis #3</i>	25
<i>Summary for hypothesis #4</i>	26
<i>Summary for hypothesis #4</i>	31
<i>Summary for hypothesis #5</i>	32
Citations	36
Appendix	38
Presentations and Student Data Products	38
Quality Assurance Project Plan.....	39

Executive Summary

The objective of this project was to increase our understanding of cyanobacterial harmful algal blooms (HABs) in NJ lakes, addressing a core need in the state to understand the environmental conditions driving the formation of HABs. Here, the focus was on coastal lakes, principally Deal Lake (and the hydrologically linked Sunset Lake) in Monmouth County, NJ. Coastal lakes differ from other NJ lakes in that they have a connection to the ocean. Two important consequences of this are (1) coastal lakes have higher salinity and conductivity than typical inland lakes, and (2) coastal lakes discharge at ocean bathing beaches, potentially delivering cyanobacteria plumes and their toxins when HABs are present in the lake. A combination of traditional and innovative genomics-based techniques were used to examine water quality and HAB dynamics, as well as their relationship to upper trophic level community structure.

Project objectives / hypotheses / summary results:

1. Are the sampled stations around Deal and Sunset Lakes different from each other in terms of HAB biomass and/or toxicity over the time-period covered?

Yes. Stations around Deal Lake differ significantly according to the physical, chemical, and biological measurements made in this study. This underscores the need to consider spatial variability when designing monitoring plans, even for relatively small lakes such as Deal Lake.

2. Do cyanobacteria and/or cyanotoxins contaminate ocean swimming beaches during bloom periods?

While a Deal Lake ‘signature’ in terms of chemical / physical / biological properties was found at the outfall beach for Deal Lake, the signature appears to be diluted quickly. Further study is required to understand this dynamic including continuous sampling through flood conditions.

3. Does the abundance or ratio of cyanobacterial / toxin genes (measured by quantitative PCR - qPCR) predict cyanotoxin levels determined by the ELISA (Enzyme Linked Immunosorbent Assay) method?

An analysis of 195 paired qPCR – ELISA samples spanning 2021 – 2023 showed statistically significant positive correlations between qPCR results and toxin concentrations for both microcystin and saxitoxin.

4. What does cyanobacterial composition of Deal and Sunset Lakes look like when measured via 16S metabarcoding? How does this compare to microscope determinations of community composition?

16S metabarcoding produced reasonable estimates of cyanobacterial community composition that showed significant seasonal variability, and changing community composition during documented HAB events. Comparisons with microscope estimates showed some similarities and some discrepancies related to

the inherent biases of each methodology.

5. Does rainfall predict HAB events or the expansion of a HAB in Deal and Sunset Lakes?
Results for near-term rainfall (1-14 days before sampling) in Deal Lake showed positive relationships between Dissolved Inorganic Nitrogen (DIN) and PO₄ and rainfall, while near-term rainfall was negatively correlated to HAB biomass in Deal Lake. DIN, PO₄ and HAB biomass showed no relationship to rainfall in Sunset Lake. This supports the idea that rainfall runoff is a significant source of nutrients to Deal Lake, and although hydraulically connected, the HAB events that occur in both bodies of water are likely independent of one another.
6. Are there relationships between water quality parameters (including HABs) and teleost fish in these coastal lakes that indicate potential impacts across trophic levels?
Measurements of fish community composition made via eDNA 12S metabarcoding showed (1) differences between Deal and Sunset Lake, and (2) statistically significant correlations between gene read abundance and environmental parameters, including an indicator of cyanobacterial HAB biomass for some taxa.

The scale and complexity of scientifically understanding NJ HABs and monitoring NJ lakes for potential hazards due to cyanobacterial HABs is immense and demands innovative approaches. Negative impacts of HABs include degraded water quality and toxin production, both of which can in turn negatively impact higher trophic levels and humans (Feng et al. 2024). Recently, the US White House issued a National Aquatic Environmental DNA Strategy¹ that calls for further adoption of eDNA-based genomics approaches in our nation's biodiversity monitoring programs. Here, innovative genomics approaches were integrated with an ongoing monitoring plan for coastal lakes, including qPCR detection of cyanobacterial biomass and toxin genes, and environmental DNA metabarcoding of 16S and 12S genes to measure bacterial and teleost fish community composition, respectively. This allows us to exam both the dynamics of bacterial populations, including potentially toxic cyanobacterial HABs, as well as fish communities that may be impacted by HABs either directly or indirectly through degraded water quality (Lopez et al. 2008). Where possible, eDNA approaches were paired with standard or conventional quantitative methods: ELISA was used to quantitatively measure the total toxin amount in each sample, and quantitative enumeration (cell counts) were paired with the data collected with the 16s rRNA amplification. This permitted comparison of traditional techniques with genomics techniques that may lead to more robust and efficient monitoring strategies. 12S fish surveys were not paired with capture surveys in this study, but we have published comparisons with trawl surveys using the same protocol applied here, demonstrating strong concordance between metagenomic and capture results (Stoeckle et al. 2020, 2022). Applying genomics approaches to simultaneously examine microbial and fish community composition through metabarcoding, in

¹ <https://bidenwhitehouse.archives.gov/wp-content/uploads/2024/06/NSTC-National-Aquatic-eDNA-Strategy.pdf>

the context of other water quality measurements, provided data from which potential HAB impacts on upper trophic level organisms could be examined.

Overall, results here provide a scientific rationale for building out the genomics capability of New Jersey Department of Environmental Protection (NJDEP) for HAB science & research as well as monitoring. A key advantage of doing this would be the scalability of genomics approaches and ability to apply the same methodologies to monitoring widely disparate environments. The challenge would of course be incorporating these new metrics of cyanobacterial biomass and toxins into the currently used monitoring standards. Nonetheless, a broad recommendation stemming from this study would be to expand genomic-based research approaches to enhance ongoing monitoring programs using largely traditional methodologies, which in the case of HAB monitoring would include cell counts and ELISA toxin measurements.

Introduction

The objective of this project was to increase our understanding of cyanobacterial HABs in NJ lakes, addressing a core need in the state to understand the environmental conditions driving the formation of HABs. Additionally, development of a HAB-risk index for different NJ lakes, based on measurements of HAB biomass, toxicity and environmental drivers, is desirable. In this portion of the Multi-Purpose Grant (MPG) led by Dr. Robert Newby (NJ DEP), Monmouth University focused on coastal lakes, principally Deal Lake and Sunset Lake) in Monmouth County NJ. Coastal Lakes differ from other NJ lakes in that they have a direct or indirect connection to the ocean. Two important consequences of this are (1) coastal lakes have higher salinities/conductivity than typical inland lakes, and (2) coastal lakes discharge at ocean bathing beaches, potentially delivering cyanobacteria plumes when HABs are present in the lake.

Some of the history of Deal and Sunset Lake is covered in the Deal Lake watershed protection plan (Souza 2011). Briefly, Deal Lake is the largest coastal lake in the state of NJ, with a total surface area of 155 acres (0.63 km²), average depth of 1.8 m, a watershed area of 4400 acres (17.8 km²) that is classified as “highly urbanized” (Souza 2011), and a trophic status classified as “eutrophic” by previous investigations (Tiedemann et al. 2009). Seven NJ municipalities border Deal Lake with a combined population of approximately 70,000. Deal Lake is characterized by an eastward main basin adjacent to the Atlantic Ocean coastline that tapers to multiple tributary “arms” to the west (Souza 2011). The lake remains connected to the Atlantic Ocean via a flume gate used to regulate lake level, as well as to allow migratory fish movements into and out of the lake (Souza 2011). Deal Lake’s main basin has a volume of $0.9 \times 10^6 \text{ m}^3$, and receives annual inputs of $8.1 \times 10^6 \text{ m}^3$ from tributaries and $1.9 \times 10^6 \text{ m}^3$ from stormwater annually (Souza 2011). Sunset Lake is located within Asbury Park, has a smaller (94 acres (0.38 km²)) watershed area than Deal Lake and is hydrologically connected to Deal Lake through an overflow pipe designed to move runoff to Deal Lake during storm events (Souza 2011). Despite the descriptions of ‘degraded’ water quality (Tiedemann 2009, Adolf et al. 2022), community members value their presence, use the lakes for activities including fishing, crabbing and boating, and work actively to maintain and restore these and other coastal lakes in Monmouth County, NJ.

Methodology and QAPP

This study was conducted under an approved Quality Assurance Project Plan (QAPP, contract SR23-10), which contains the methodology and protocols used. The approved QAPP is included as an Appendix to this report.

Study Area

Fig. 1A shows a map of sampling stations. Fig. 1B illustrates the number of values present in the database for each sampling parameter by sampling station, with lighter colors indicating a greater number of data points. The sampling period under consideration here is June 1, 2021 through Nov 30, 2023.

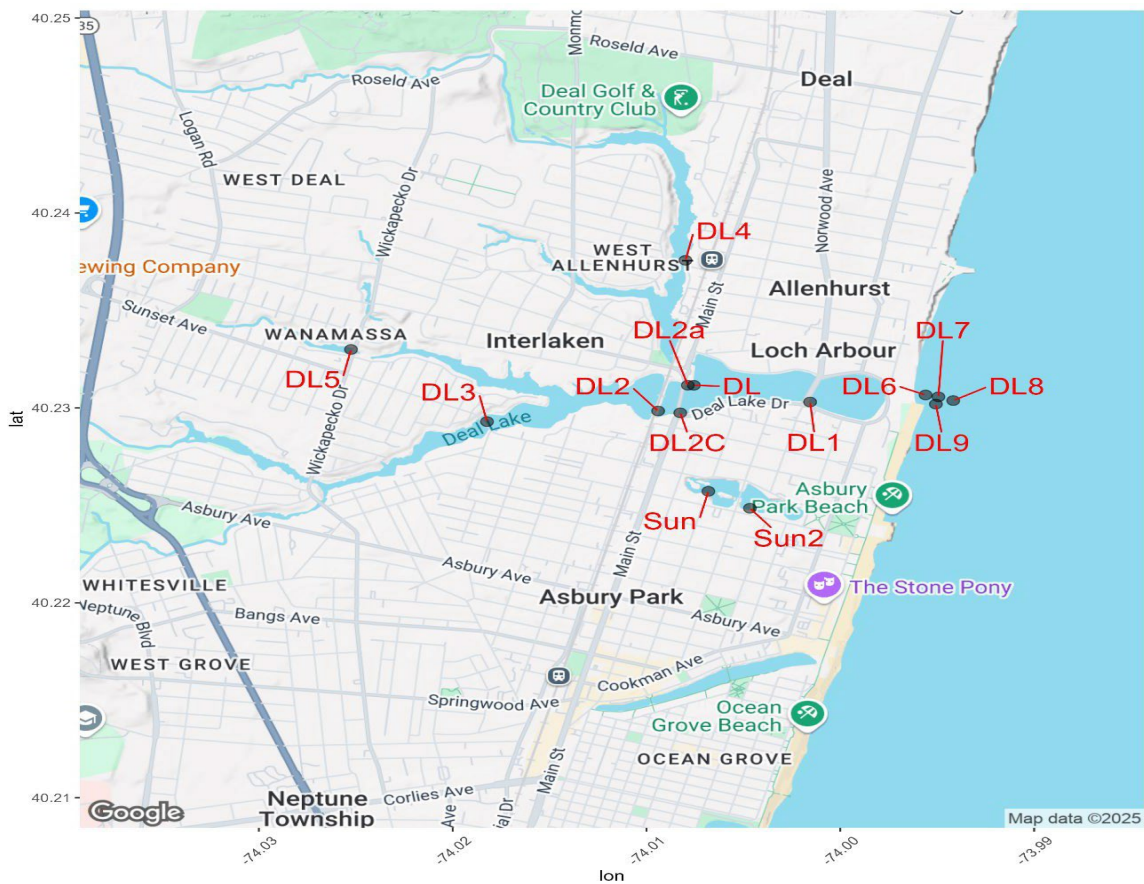


Fig. 1 (A) Sampling locations on Deal Lake (DL) and Sunset Lake (Sun).

B

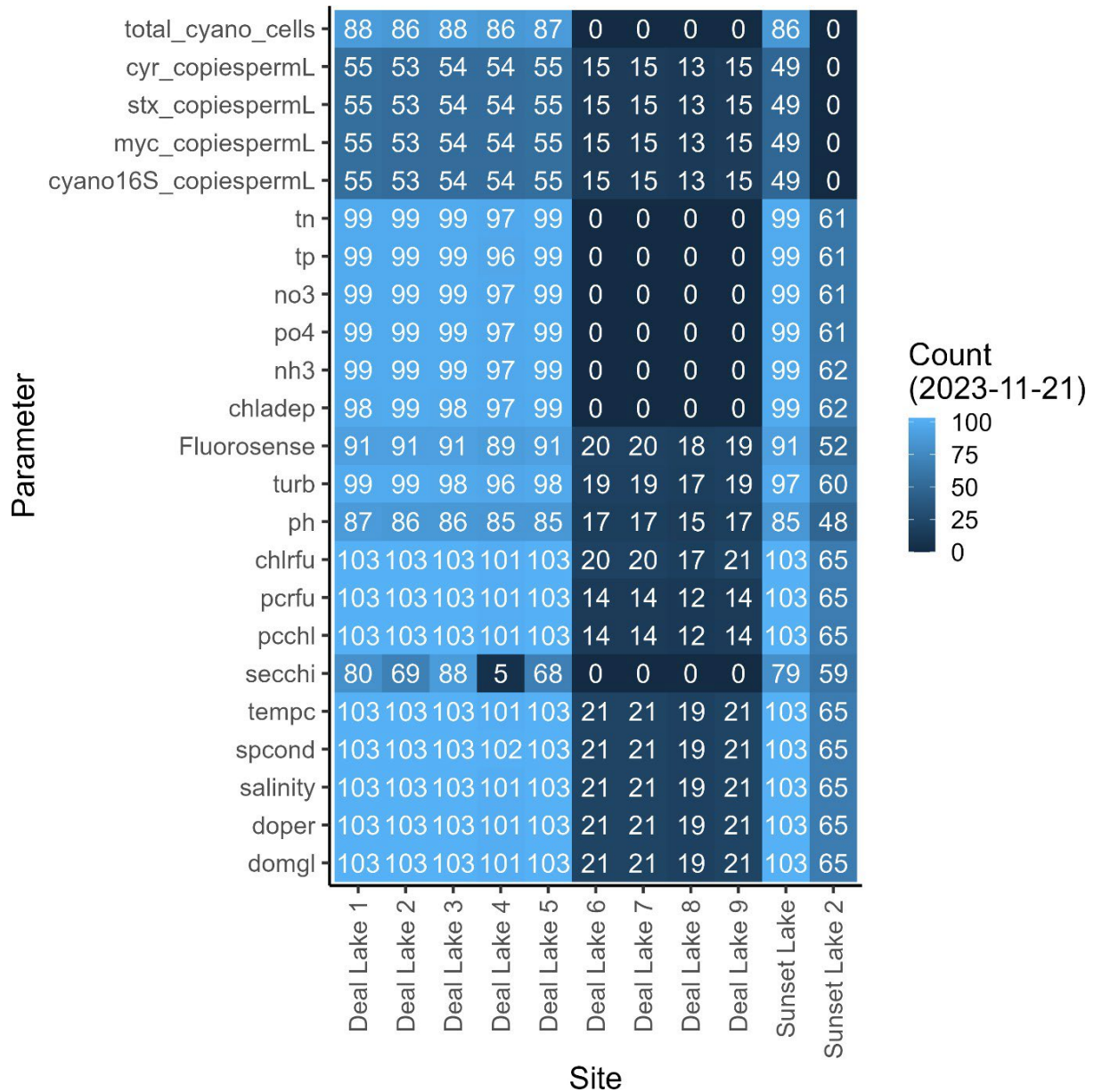


Figure 1(B) Sample inventory matrix by station and parameter (total_cyano_cells: total cyanobacterial cell count; cyr_copiespermL: qPCR results for cylindrospermopsins gene; stx_copiespermL: qPCR results for saxitoxin gene; myc_copiespermL: qPCR results for microcystin gene; 16S_copiespermL: qPCR results for cyanobacterial 16S gene; tn: total N; tp: total P; no3: nitrate + nitrite; po4: phosphate; nh3: ammonium; chldep: extracted Chl a; Fluorosense: phycocyanin fluorescence (Turner Fluorosense); turb: turbidity; pH = pH; chlrfu: chlorophyll fluorescence (Turner cyanofluor); pcrfu: phycocyanin fluorescence (Turner Cyanofluor); pcchl: ratio of pcrfu:chlrfu; Secchi: Secchi disk depth; tempc: water temperature; spcond: specific conductivity; salinity: salinity; doper: dissolved oxygen (percent saturation); domgl: dissolved oxygen (mg/L))

Field Measurements and sample collections

All samples were collected in 1 L amber acid-washed bottles. Sites were selected based on existing NJDEP field stations or proximity to possible outlet release points, as outlined in Table 1. The sites (except DL6 – DL9) were visited bi-weekly Dec – Mar, then weekly Apr – Oct. DL6 – DL9 were sampled opportunistically between June – Aug. Samples were collected and processed for both field water parameter measurements, algal collections, toxin measurements, and eDNA analysis. Sites represent surface water grabs (0.3 meters below surface) unless otherwise denoted throughout the text.

Table 1. Location, Waterbody, GPS coordinates (decimal degrees) and abbreviation ('sta_abb') of stations sampled in this report. All samples were taken as surface grab samples.

Location	Waterbody	Lat	Long	sta_abb
Deal Lake 1	Deal Lake	40.230302	-74.00156	DL1
Deal Lake 2	Deal Lake	40.229843	-74.0094	DL2
Deal Lake 2a	Deal Lake	40.2311623	-74.0078685	DL2a
Deal Lake 2C	Deal Lake	40.229746	-74.008259	DL2C
Deal Lake 3	Deal Lake	40.229294	-74.018229	DL3
Deal Lake 4	Deal Lake	40.237572	-74.00799	DL4
Deal Lake 5	Deal Lake	40.232996	-74.025247	DL5
Deal Lake 6	Deal Lake	40.230664	-73.995602	DL6
Deal Lake 7	Deal Lake	40.230568	-73.994943	DL7
Deal Lake 8	Deal Lake	40.230376	-73.994176	DL8
Deal Lake 9	Deal Lake	40.230196	-73.995073	DL9
Deal Lake	Deal Lake	40.23116	-74.00756	DL
Sunset Lake	Sunset Lake	40.22572	-74.00681	Sun
Sunset Lake 2	Sunset Lake	40.224851	-74.004665	Sun2

Water parameters measured by field staff were phycocyanin (PC), chlorophyll (Chl a), dissolved oxygen (D.O.), salinity, specific conductance (spcond), temperature, and turbidity (turb). Briefly, a clean bucket rinsed with site water three times (3X) was filled on location and allowed to settle. Measurements were collected and recorded from this container.

Water for nutrient analyses was collected in 1 L brown High-Density Polyethylene (HDPE) bottles that have been acid washed and rinsed with distilled water (dH₂O) and then rinsed with site water. These bottles were capped and stored on ice until they were driven (within 4 hours of collection) to the NJDEP Bureau of Marine Water Monitoring Leeds Point Laboratory for nutrient analysis. Upon arrival at the laboratory, the samples were preserved in accordance with the laboratory's current standard operating procedures (SOPs). Samples processed by the NJDEP Bureau of Marine Water Monitoring Leeds Point Laboratory were analyzed for Total Nitrogen (TN), Total Phosphorous (TP), Dissolved Inorganic Nitrogen (DIN), and Dissolved Inorganic Phosphorous (DIP).

Algal Analysis

20 mL samples were aliquoted from the above-collected water samples and preserved with 5% (final by volume) acidified Lugol's Iodine. These samples were stored at ambient temperature in a dark condition inside a laboratory cabinet prior to enumeration using Monmouth University SOPs. Both cell identification and enumeration occurred with a Sedrick-Rafter style chamber using an inverted compound light microscope (Nikon Diaphot 300). Random grid counting was performed, and natural units were enumerated for phytoplankton. Counts for individual species/natural units are done on five randomly chosen grids per slide then averaged.

Cyanobacteria taxa were grouped based on presenting morphological features (colonial, filamentous, unicellular) and identified to genus level. Samples or photos were sent to the NJDEP Division of Science and Research for confirmation analysis or phycological keys were consulted for identification of species.

Quantitative gene analysis (qPCR) for 16s and toxin genes in cyanobacteria

50mL water samples were collected in DNA/RNA free lot certified plastic centrifuge tubes and stored on ice until being filtered onto 25 mm nitrocellulose filters using an acid-washed and rinsed 60 mL syringe with filter holder. 20 mL of this sample was used as described here for qPCR samples, while the remainder (30 mL) was filtered for metabarcoding as described below. Forceps used to transfer filters from filter caps to 2 mL sterile screw cap microcentrifuge tube were rinsed with 10% bleach followed by dH₂O in between samples. Samples were stored at -80°C until being analyzed by qPCR.

The Cyano D-Tec qPCR assay (Phytoxigene, Inc., 526 S. Main St., Suite 714B, Akron, OH 44311) for total cyanobacteria and cyanobacterial toxin genes is used according to the manufacturer's guidance. Samples are mixed with a reaction mix supplied by the manufacturer which contains the polymerase, primers, deoxynucleotide triphosphates (dNTPs), internal amplification control (IAC), and buffer). A no template control (NTC) is set up which does not contain sample as a reaction control to ensure that there is no molecular carry over between samples or contamination present. This work is carried out in a dedicated certified laminar airflow hood, with molecular grade water, and DNA/RNA free, DNAase/RNAase filtered tips, and micropipettes which are UV sterilized prior to use. The qPCR assay contains an internal amplification control which allows detection of PCR inhibitors in DNA extracts, a common occurrence when running PCR on environmental DNA extracts. Our initial tests using Deal and Sunset Lake DNA extracts showed that PCR inhibitors were present in many samples. To alleviate this, DNA extracts were diluted 1:10 with molecular grade water prior to addition as template in qPCR. All results are presented as gene copies per mL, per manufacturer's specification. The Cyano D-Tec qPCR assay measures total cyanobacteria through the 16S gene, microcystin toxin gene (*mycE/ndaF*), cylindrospermopsin toxin gene (*cyrA*), and saxitoxin gene (*stxA*) presence and abundance. A QuantStudio5 (Thermo Fisher Scientific) qPCR instrument was used to run the samples.

eDNA sample collection and processing

The process of using eDNA for bacterial and fisheries (Stoeckel et al. 2020) surveys may be broken into three steps detailed below: Water collection, filtration and processing (including sequencing), and bioinformatic analyses.

Water Collection

30 mL of the eDNA water sample collected as described above in the qPCR section was used for metabarcoding samples.

Filtration and Processing

The water sample was poured into a glass filter manifold attached to wall suction with a 47-mm, 0.45µm pore size nitrocellulose filters (Millipore) installed. Filters were folded to cover retained material and stored in sterile 15-ml tubes at 80°C. As negative controls for each sample set, a 30 mL sample of laboratory tap water was filtered using the same equipment and procedures, and on the same day as for field samples. Total DNA extraction was carried out using the Qiagen PowerWater DNA extraction kit. Blank filters (tap water) were processed with samples as controls. DNA quantity and quality was determined spectrophotometrically (ThermoFisher NanoDrop 2000) on a 1 µL sub aliquot of the extract. DNA extracts were stored in an alarmed - 80 °C freezer until further analyses.

Molecular analysis

PCR was used to generate amplicons for metabarcoding, using two primer sets (separately): The V4 region of the 16S gene for bacteria (Caporaso et al. 2011) and the 12S region for vertebrates including fish (Riaz et al. 2011).

Table 2. Primer sequences used for amplicon generation for Illumina sequencing.

Assay	Primer sequence	reference
V4 16S	Forward: 5'- TCGTCGGCAGCGTCAGATGTGTATAAGAGACAGGTGYCAGCMGCCGCGGTAA-3'	Caporaso et al. 2011
V4 16S	Reverse: 5'- GTCTCGTGGGCTCGGAGATGTGTATAAGAGACAGGGACTACNVGGGTWTCTAAT-3'	Caporaso et al. 2011
12S	Forward: 5'- TCGTCGGCAGCGTCAGATGTGTATAAGAGACAGACTGGGATTAGATACCCC-3'	Riaz et al. 2011
12S	Reverse 5'- GTCTCGTGGGCTCGGAGATGTGTATAAGAGACAGTAGAACAGGCTCCTCTAG-3'	Riaz et al. 2011

Amplicon quality was checked by agarose gel electrophoresis to ensure the expected fragment size was present after PCR. Upon satisfactory gel electrophoresis, a 20-fold diluted (in molecular grade water) aliquot of the PCR product was shipped to the BioAnalytical Services Laboratory (BASLab) at the University of Maryland Institute for Marine and Environmental Biotechnology for DNA library building, and Illumina sequencing (Illumina MiSeq platform) according to their own standard protocols. Products of this service included de-multiplexed FastQ files, which were then processed further.

Bioinformatics and biodiversity analyses

Bioinformatic analyses to determine amplicon sequence variants (ASVs – the unique sequence variants contained within the sequence reads resulting from Illumina sequencing) was done in the R package DADA2 (Callahan et al. 2016). ASVs were matched to taxonomic reference

databases (Silva, <https://www.arb-silva.de/> for bacteria; custom database for 12S Riaz primers) with DADA2. This resulted in ‘taxa tables’ with DNA reads per taxon per sample that were used to determine presence / absence as well as relative abundance (based on relative read abundance within a sample).

Metabarcoding data were summarized in two ways in this report, using R statistical programming language and R Studio IDE. For each dataset, taxa (determined as ASVs or amplicon sequence variants) are shown in heat maps (by season and station) showing the proportion of samples in which they were detected above a threshold of 10 sequences per sample. These same data are shown as an nMDS ordination (using relative read abundance within a sample as the ‘abundance’ metric for each ASV) color-coded by season and station to examine whether or not such samples have a similar bacterial community composition. Additionally, k-means clustering (using partitioning around medioids (PAM)) was run on the 16S dataset (including all bacteria) to summarize differences in community composition. K-means clustering is a machine learning algorithm that identifies and labels ‘clusters’ within high dimensional data based on an algorithm that looks to minimize within cluster variance while maximizing between cluster variance. Since the dimensionality of metabarcoding data is ‘taxa’, clusters determined here represent different community composition types within the data.

Data Inventory

Data in the master dataset (“epa_proj_out.csv”) has been indexed to cumulative rainfall for the region, based on <https://njdep.rutgers.edu/rainfall/> data for the Monmouth County coastal lakes region. A metadata file is also included that contains column explanations.

Environmental DNA (eDNA) samples from select times / locations were collected and submitted for Illumina Miseq sequencing following amplification by 16S V4 515F 806R primers (Caporaso et al., 2011). Bioinformatic analyses used DADA2 (Callahan et al. 2016) with Silva v. 138.1 as a reference database. A total of 196 samples (including controls) were analyzed in this way (2021 - 2023). The taxa tables for these samples are contained in “clonet_16s_all.csv”.

A subset of DNA extracts used for 16S metabarcoding (total of 69 samples) were also analyzed by 12S metabarcoding using Riaz (Riaz et al. 2011) teleost primers to inventory fish (and other vertebrate) sequences for Deal Lake and Sunset Lake. Bioinformatics for these samples was done in DADA2 using a custom database (Stoeckle et al. 2020). These data are in the dataset “clofish_df_all1.csv”.

A total of 195 samples (2021 – 2023) were sent to NJ DEP for ELISA analysis of cyanotoxins and comparison with qPCR results. These data have been indexed to lake samples in “epa_proj_out.csv”.

All data sets mentioned above as well as all analyses and outputs shown below are available in an R project format upon request. R projects are self-contained directories with all code, data inputs, graphical or data outputs. R projects are meant to be able to be run on any computer running R Studio IDE.

Results

1. Are the stations (DL1 – DL5, Sunset) different from each other in terms of HAB biomass and/or toxicity over the time-period covered?

Examination of phycocyanin fluorescence, which measures the pigment phycocyanin in the phycobilisome of cyanobacteria and rainfall time series for the project stations and time period (Fig. 2) sets the stage for analyses of these data and shows differences by site and lake. The time series began Jan 1, 2021 in order to show leading samples and rainfall before the actual project start date in May 2021. In general, summer of '22 and '23 saw larger cyanobacterial blooms than summer of '21 (discussed later in the report), with stations DL 4 & 5 (located to the west) showing less cyanobacterial activity than other more eastern stations (DL 1 – 3). The Deal Lake '22 & '23 bloom peaked in July, whereas the Sunset Lake '22 bloom peaked in September (showing very little activity in July) and the Sunset Lake '23 bloom started before June and re-peaked in July. July '22 was a dry period with little rain, shown by the lack of grey bars on the graphs. This dry spell continued through September until Hurricane Ian (Sept 23 – Sept 30, 2022) dumped approximately 4" of rain on the region coinciding with a drop in cyanobacterial concentrations at all stations. Summer of '23 was dry through June by rain did occur in July. In summary, stations DL1 – DL4 had similar annual phycocyanin (PC) dynamics, with DL5 being different in that very little PC was detected. Sunset Lake showed different PC dynamics from DL1 – DL4, particularly in summer '22 when the timing was different.

To address this hypothesis, parameters were compared among the main sampling sites (DL1 – DL5, SUN1-2. Please see Fig. 1). Analyses including DL6-9 (ocean sites) will be included elsewhere (please see Fig. 7 – 9) since they were not sampled as consistently as the main sites (these ocean sites were sampled Aug / Sep 2021; Jun – Aug 2022; and May – Aug 2023). For each plot, the results from a non-parametric Kruskal-Wallis are shown, along with the total number of observations and date range for data on each plot. The reference group for the multiple comparisons (shown as asterisks) was 'all samples', e.g., compared to the overall median value of the parameter in question.

Plots comparing dissolved oxygen, specific conductivity, water temperature, and Secchi depth are shown in Fig. 3. Dissolved oxygen was relatively high at DL1, and relatively low at DL5. Specific conductivity showed a decreasing gradient from DL1 to DL5, with both Sunset Lake stations on the low end of that gradient. No differences were apparent in water temperature.

Secchi depth was relatively high at DL1, DL3 and DL5, and relatively low at Sunset 1&2.

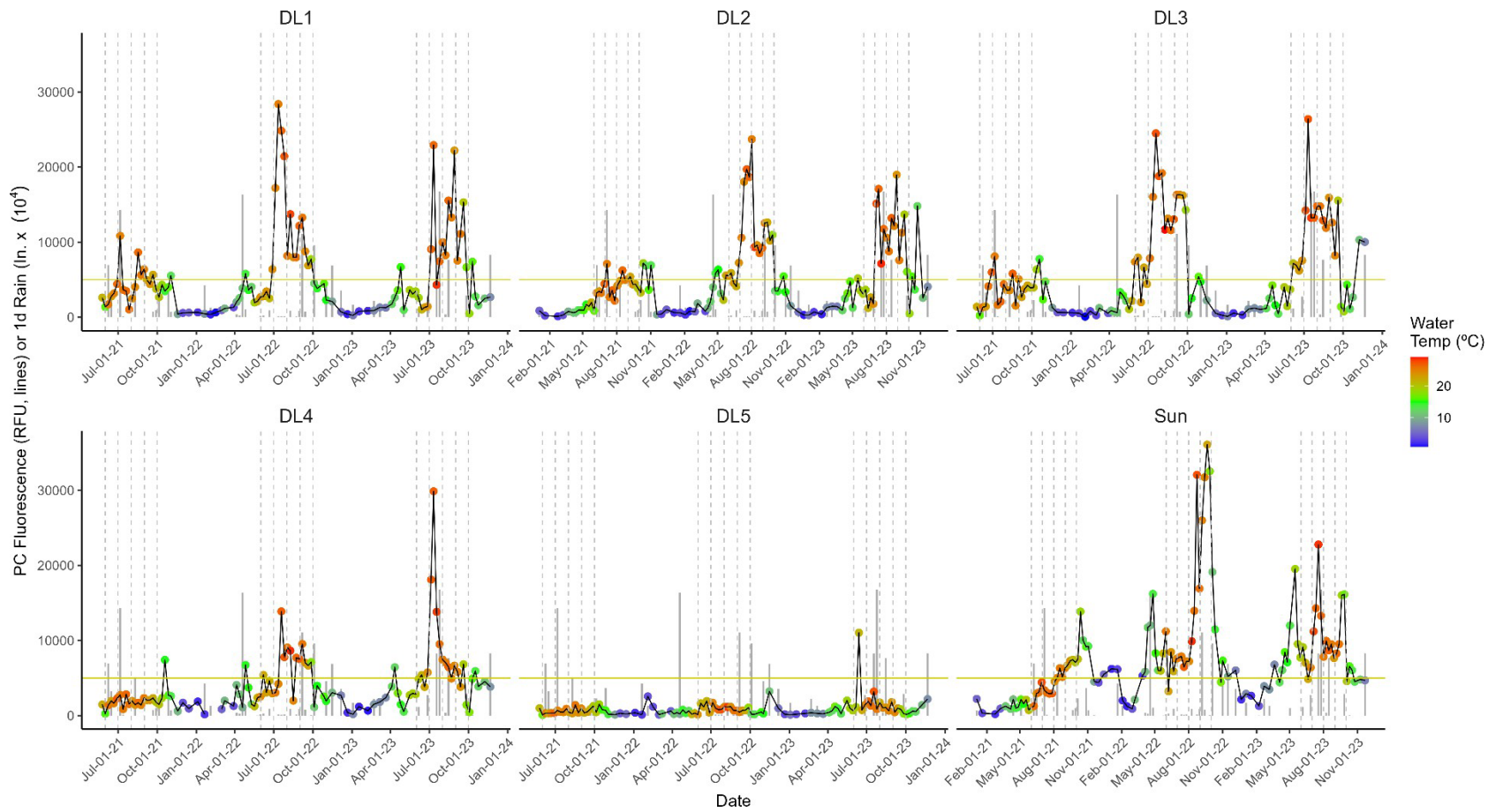


Fig. 2 Phycocyanin (PC) fluorescence (RFU) (point and lines) and rainfall (bars) time series by station. The color of each point is coded for water temperature at the time of measurement. Dashed vertical lines are the 1st day of each month of the ‘HAB season’ (June – Oct).

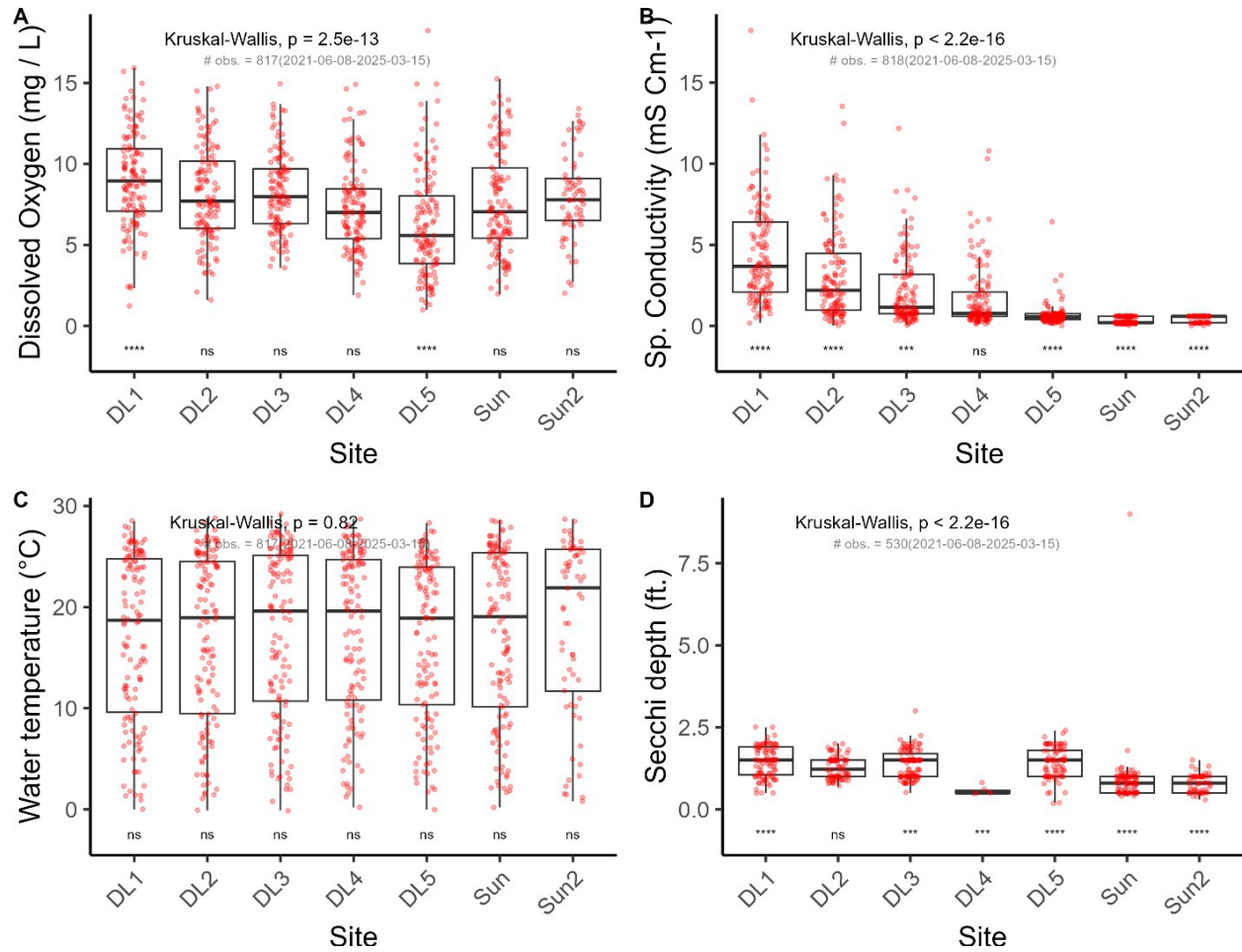


Fig. 3 Physical and chemical water quality parameters by sampling station. Within each box, the centerline represents the median value while the lower and upper box limits represent the inter-quartile (25th – 75th) range. Whiskers extends from the upper and lower box bounds to 1.5*the interquartile range. The cloud of smaller dots (*jitter*) over each box represents actual measurements made at each station. On each graph the results of a non-parametric Kruskal-Wallis analysis of differences among stations (referenced to all data) is shown along with the number of observations considered. Post-hoc differences of each station relative to all data are shown above the x-axis as: ns = not significant; * = $p < 0.05$, ** = $p < 0.01$, *** = $p < 0.001$.

However, it is important to note that these Secchi depths are very low in general, as clarity in the lake is generally remarked as poor.

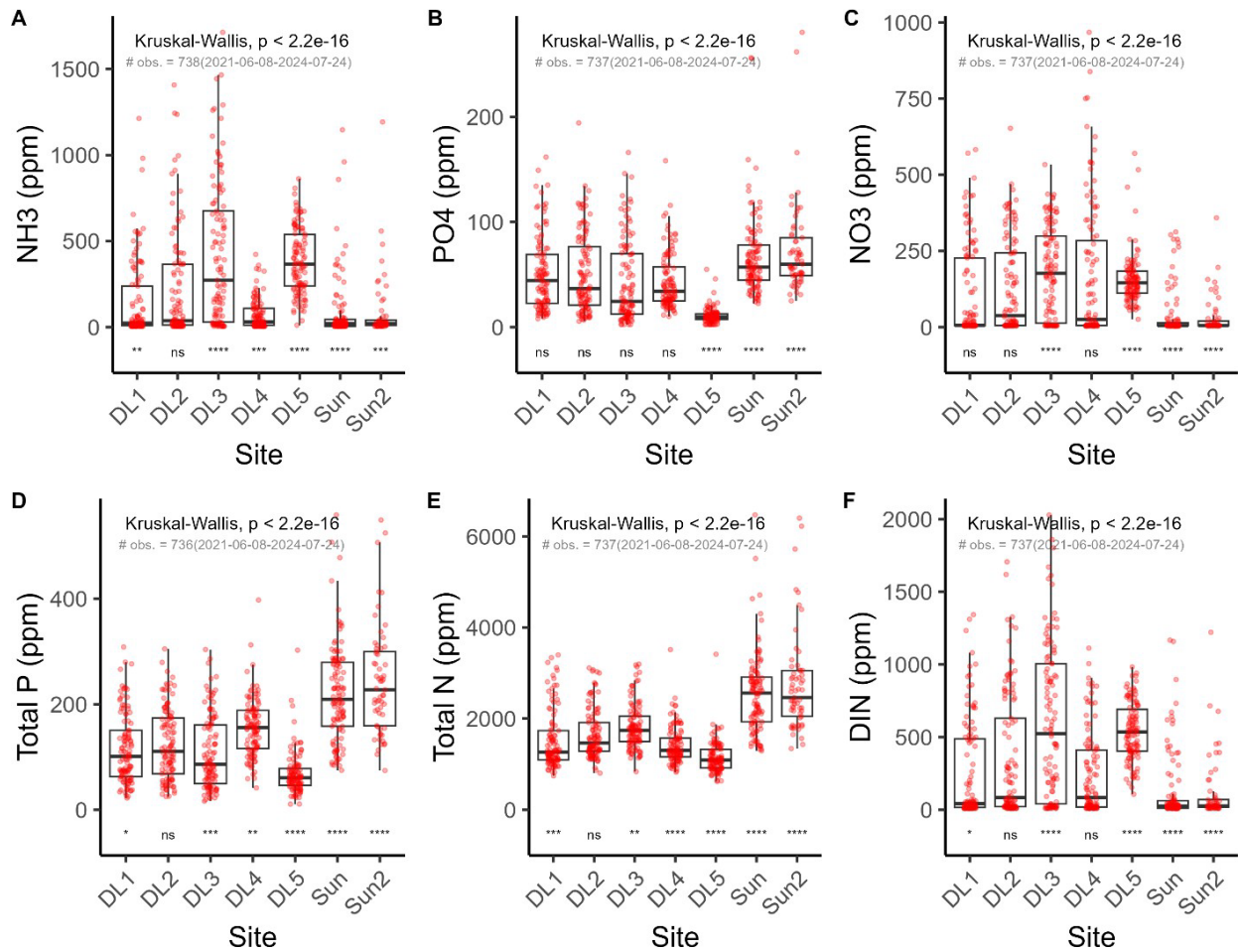


Fig. 4 Nutrient parameters by sampling station. On each graph the results of a non-parametric Kruskal-Wallis analysis of differences among stations (referenced to all data) is shown along with the number of observations considered. Post-hoc differences of each station relative to all data are shown above the x-axis as: ns = not significant; * = $p < 0.05$, ** = $p < 0.01$, *** = $p < 0.001$.

Comparisons of nutrient data among stations (Fig. 4) are complex:

- Total Nitrogen (TN) and Total Phosphorous (TP) tend to be higher in Sunset Lake than Deal Lake
 - Despite high TN in Sunset Lake, Dissolved Inorganic Nitrogen (DIN) tended to be low
- Sunset Lake stations did not differ from each other
- Within Deal Lake
 - DL5 had comparatively high DIN, including both NO_3 and NH_4
 - DL5 tended to have comparatively low TP (and PO_4)

- TN peaked at DL2 and DL3
- DL3 had comparatively high median DIN

Statistical analysis figure for select variables testing for significance at select locations for this study.

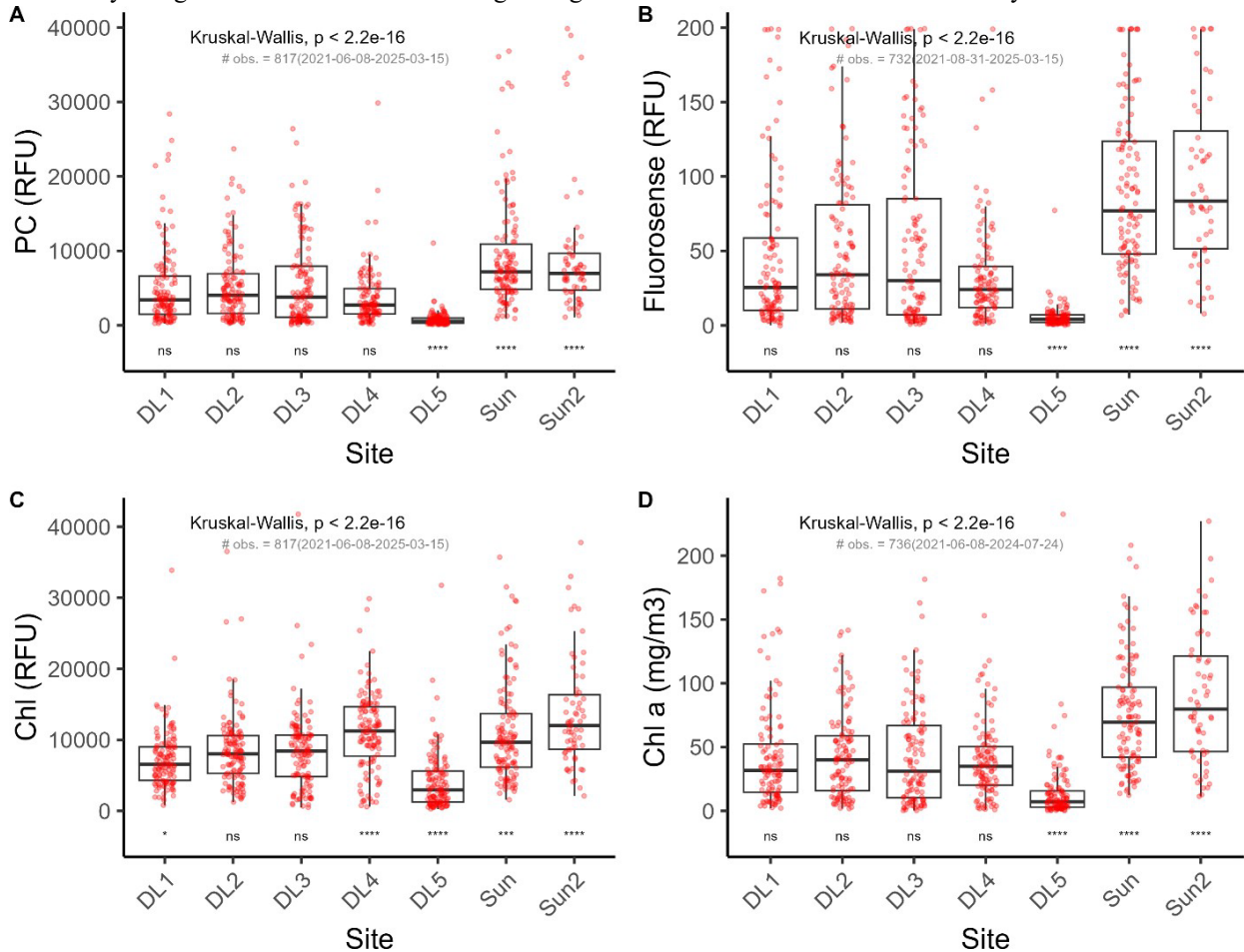


Fig. 5 Fluorometer (A, C = Turner CyanoFluor, B = Turner Fluoresence) and extracted Chl *a* (D) biomass metrics by sampling station. On each graph the results of a non-parametric Kruskal-Wallis analysis of differences among stations (referenced to all data) is shown along with the number of observations considered. Post-hoc differences of each station relative to all data are shown above the x-axis as: ns = not significant; * = $p < 0.05$, ** = $p < 0.01$, **** = $p < 0.001$.

Comparisons of biomass indices for phycocyanin (Fig. 5A, B) showed similar patterns between the Turner CyanoFluor and Turner Fluorescence, with relatively high values in Sunset compared to Deal Lake, and relatively low values at DL4 and DL5 within Deal Lake. Likewise, comparisons of CyanoFluor Chl (RFU) and extracted Chl *a* (Fig.5 C,D) also showed similar patterns among stations, with relatively high value for Sunset compared to Deal Lake, and within Deal Lake relatively low values for DL5.

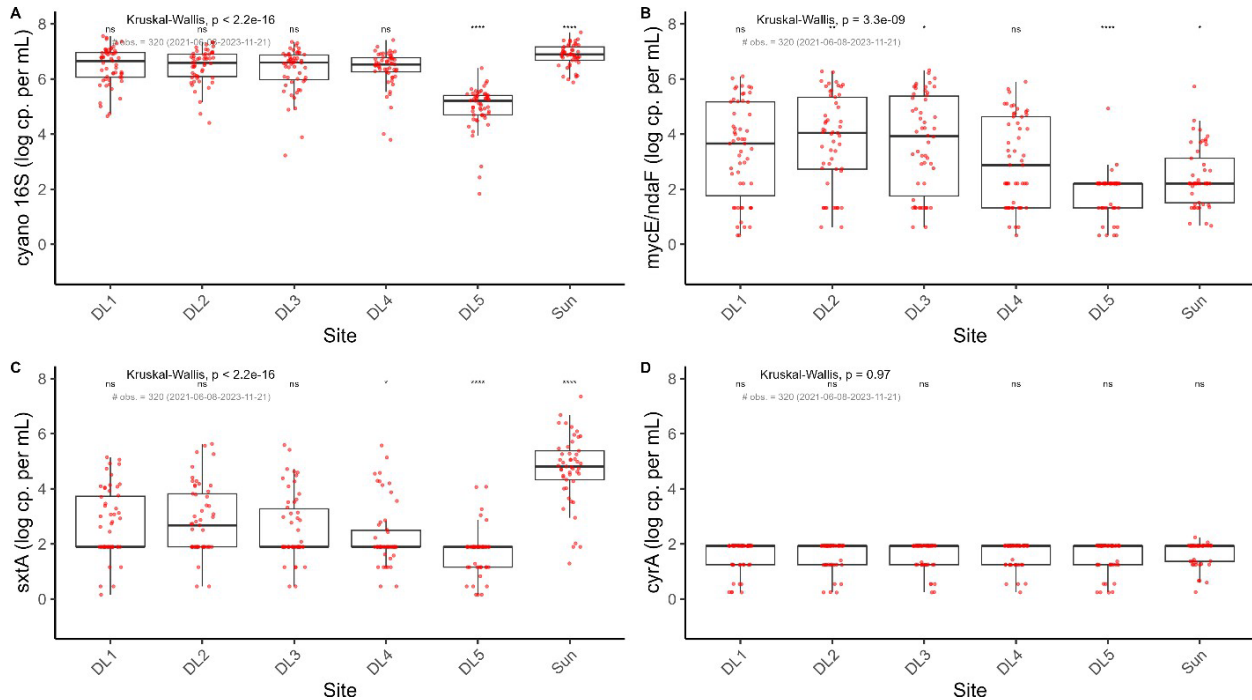


Fig. 6 qPCR parameters by sampling station. On each graph the results of a non-parametric Kruskal-Wallis analysis of differences among stations (referenced to all data) is shown along with the number of observations considered. Post-hoc differences of each station relative to all data are shown above the x-axis as: ns = not significant; * = $p < 0.05$, ** = $p < 0.01$, *** = $p < 0.001$.

Comparisons of the qPCR dataset (Fig 6) showed differences within Deal Lake and between Deal and Sunset Lakes. The abundance of 16S was relatively low at DL5 and otherwise uniform across sites in Deal and Sunset Lakes. Abundance of mycE/ndaF (marker gene for microcystin / nodularin) showed peak median value at DL2, but values were generally low across sites. By contrast, abundance of sxtA (marker gene for saxitoxin) was relatively low at DL5 and relatively high at Sunset Lake, with the other Deal Lake sites showing a pattern of decreasing abundance of sxtA moving from DL1 to DL4 (e.g. westward, away from the ocean).

Summary for hypothesis #1

With regard to the original hypothesis, we found significant differences among Deal Lake station, as well as between Deal and Sunset Lake, in key water quality parameters.

2. Do cyanobacteria and/or cyanotoxins contaminate ocean swimming beaches during bloom periods?

Fig. 7 shows water quality parameters indicative of phytoplankton and cyanobacterial biomass, and Fig. 8 shows qPCR results for cyanobacterial biomass and toxin genes, filtered for days when lake and beach stations were measured together. Comparing the values in the lake (DL1-5) with the coastal ocean transect (DL6-8) and outflow (DL9) allows us to address this hypothesis. Sunset Lake samples are shown for reference. Together, these data support the conclusion that some cyanobacterial biomass, as well as toxin genes, are exported from Deal Lake into the adjacent ocean during blooms.

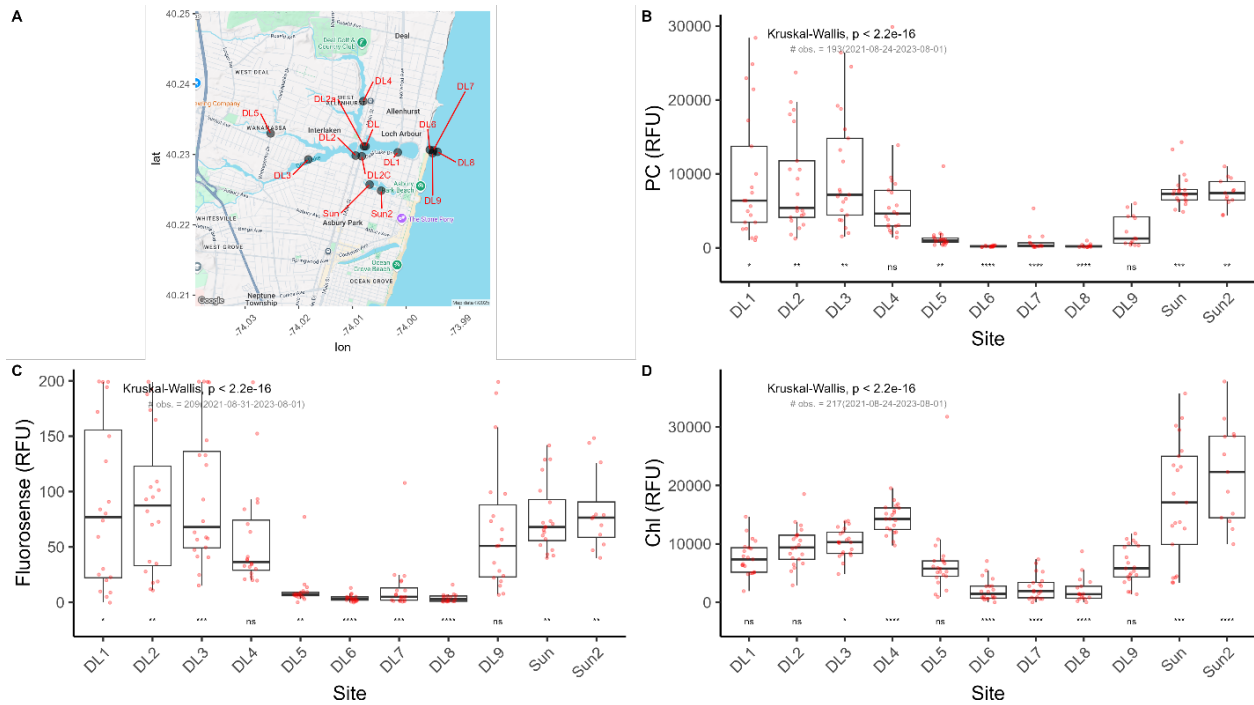


Fig. 7 Phytoplankton and cyanobacterial fluorescence parameters for beach sampling days only. On each graph the results of a non-parametric Kruskal-Wallis analysis of differences among stations (referenced to all data) is shown along with the number of observations considered. Post-hoc differences of each station relative to all data are shown above the x-axis: ns = not significant; * = $p < 0.05$, ** = $p < 0.01$, *** = $p < 0.001$.

Specifically, the influence is seen at stations DL7 and DL9, representing samples taken apx. 50' north of, and directly at the outflow, respectively. Phycocyanin fluorescence is lower than in the lake, but 16S and saxitoxin gene abundance are similar.

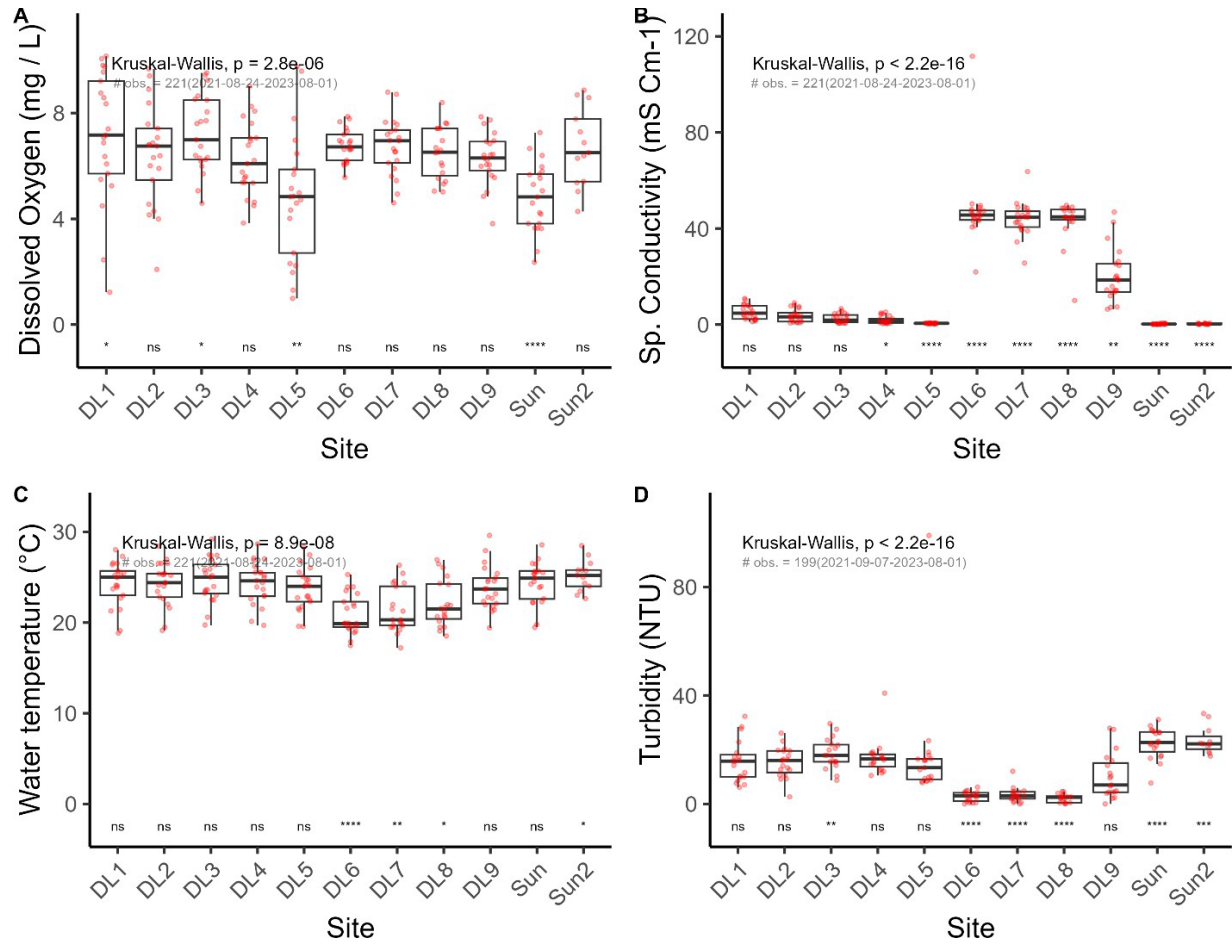


Fig. 8 Water quality parameters for beach sampling days only. On each graph the results of a non-parametric Kruskal-Wallis analysis of differences among stations (referenced to all data) is shown along with the number of observations considered. Post-hoc differences of each station relative to all data are shown above the x-axis as: ns = not significant; * = $p < 0.05$, ** = $p < 0.01$, *** = $p < 0.001$.

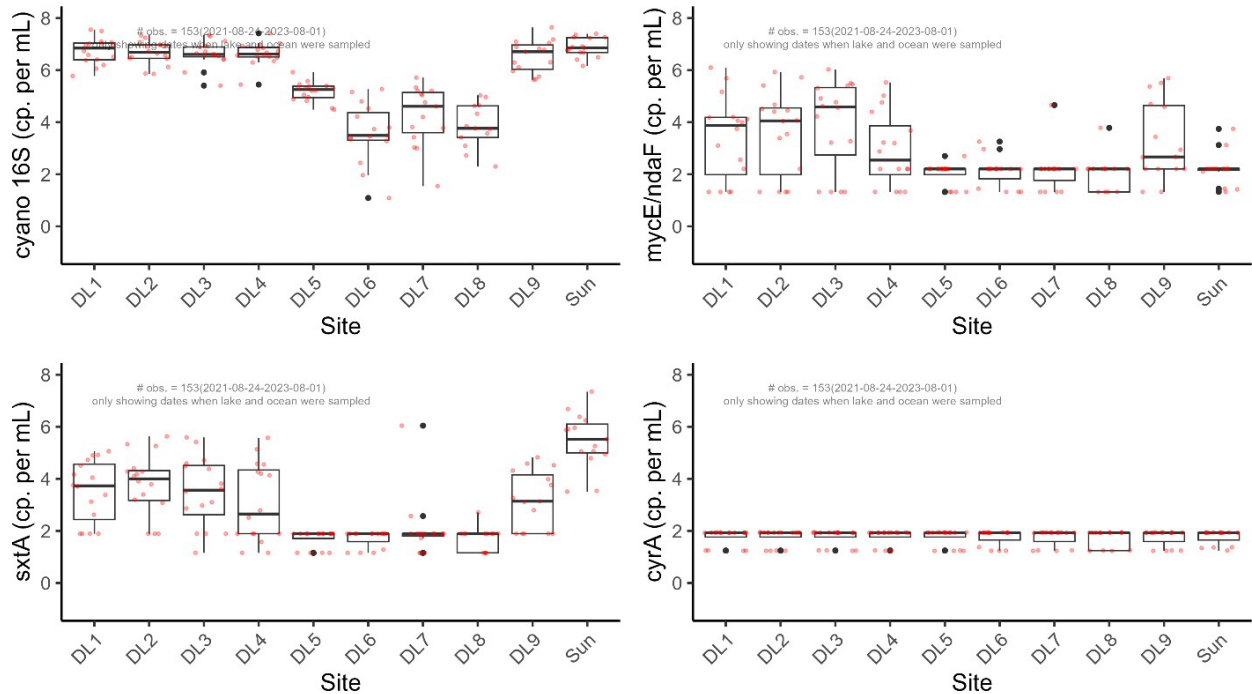


Fig. 9 qPCR parameters for beach sampling days only. On each graph the results of a non-parametric Kruskal-Wallis analysis of differences among stations (referenced to all data) is shown along with the number of observations considered. Post-hoc differences of each station relative to all data are shown above the x-axis as: ns = not significant; * = $p < 0.05$, ** = $p < 0.01$, *** = $p < 0.001$.

Summary for hypothesis #2

Water from Deal Lake reaches the outflow (station DL9) carrying cyanobacteria with it and presumably toxins, if present. However, the Deal Lake signature (in terms of cyanobacteria) was weak at stations DL6, DL7, and DL8 representing a transect from the beach out to the end of (and ~ 50 ft. north of) the groin containing the outflow. This suggests a high degree of dilution and dispersal of Deal Lake outflow water in the receiving ocean water. Further analyses targeting flood events and continuous monitoring of this phenomenon are warranted.

3. Does the abundance or ratio of cyanobacterial / toxin gene abundance predict cyanotoxin levels determined by the ELISA method?

Here, the relationship between HAB abundance indices (PC fluorescence & 16S gene abundance) is examined, as well as the relationship between qPCR results for cyano toxin genes and ELISA toxin analyses for a subset of samples. First, looking at the relationship between phycocyanin fluorescence and cell counts (Fig. 10A), as well as the relationship between 16S cyano gene copy number and cell counts (Fig. 10B), in both cases a positive correlation is seen. Phycocyanin (PC) fluorescence and Cyano 16S gene abundance were also positively correlated ($R = 0.82$, $p < 0.001$).

‘Toxicity’ of a sample, as determined through molecular assays of the toxin molecule (e.g., ELISA, HPLC, LC MS) can be difficult to define based on abundance of toxin genes in a sample because genes responsible for toxin production may or may not be expressed *in situ*. The presence of toxin genes does not always indicate that a sample is actively producing toxin. A better indicator of risk may be the use of the ratio of toxin genes to 16S genes which may indicate the relative predominance of toxic vs. non-toxic strains of cyanobacteria within an assemblage.

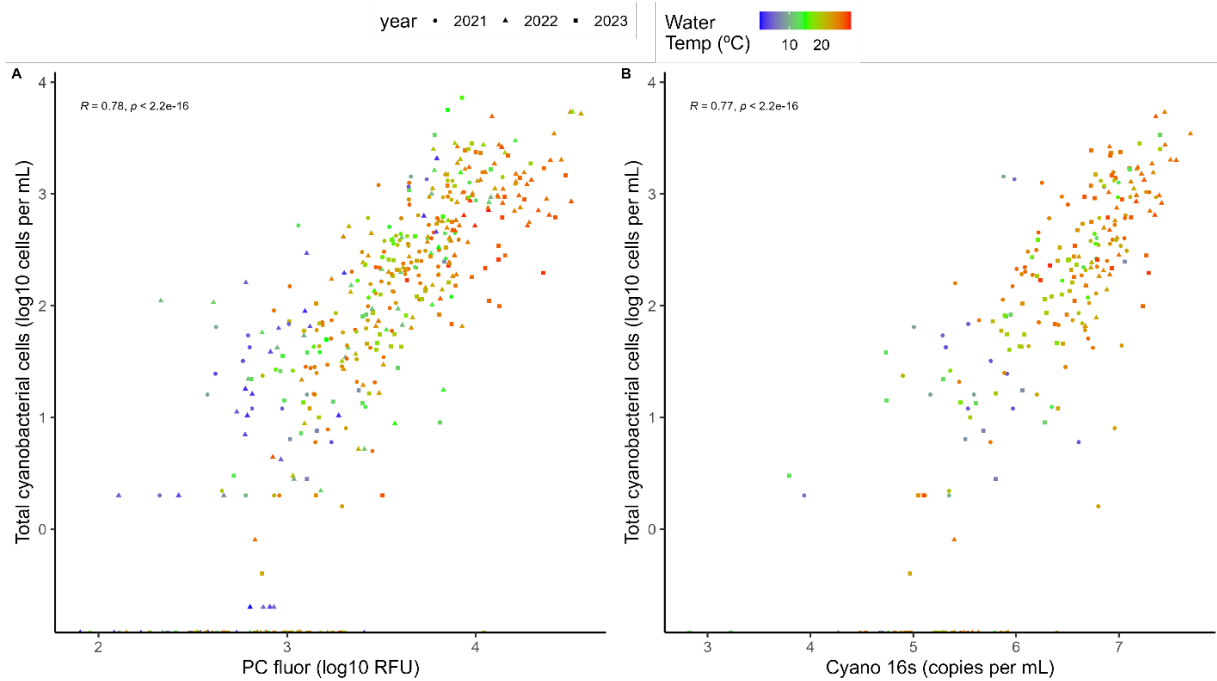


Fig. 10 Relationships between (A) PC fluorescence and total cyanobacterial cell counts and (B) cyano 16S qPCR results and total cyanobacterial cell counts. Points are colored according to water temperature. Results of a Pearson correlation are shown on each graph.

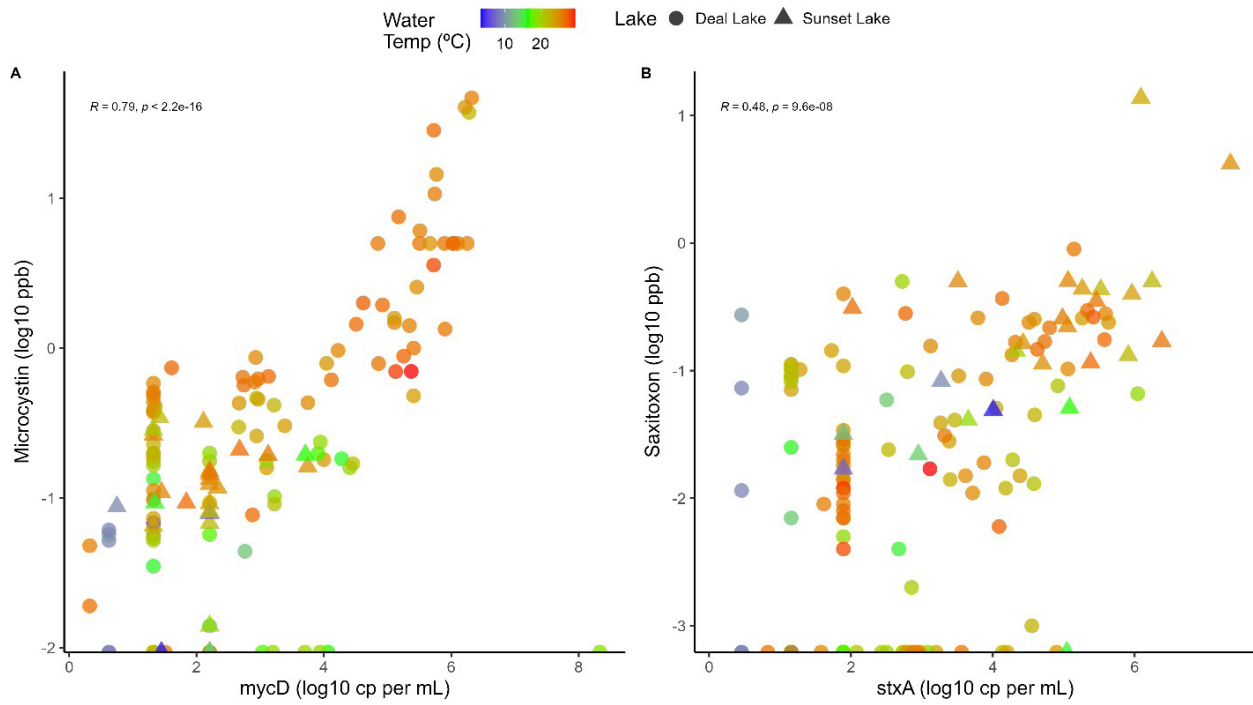


Fig. 11 Relationships between (A) mycD gene abundance as determined by qPCR and microcystin (ppb) as determined by ELISA and (B) stxA gene abundance as determined by qPCR and saxitoxin (ppb) as determined by ELISA for samples from 2021 - 2023. Points are colored according to water temperature. Results of a Pearson correlation is shown on each graph.

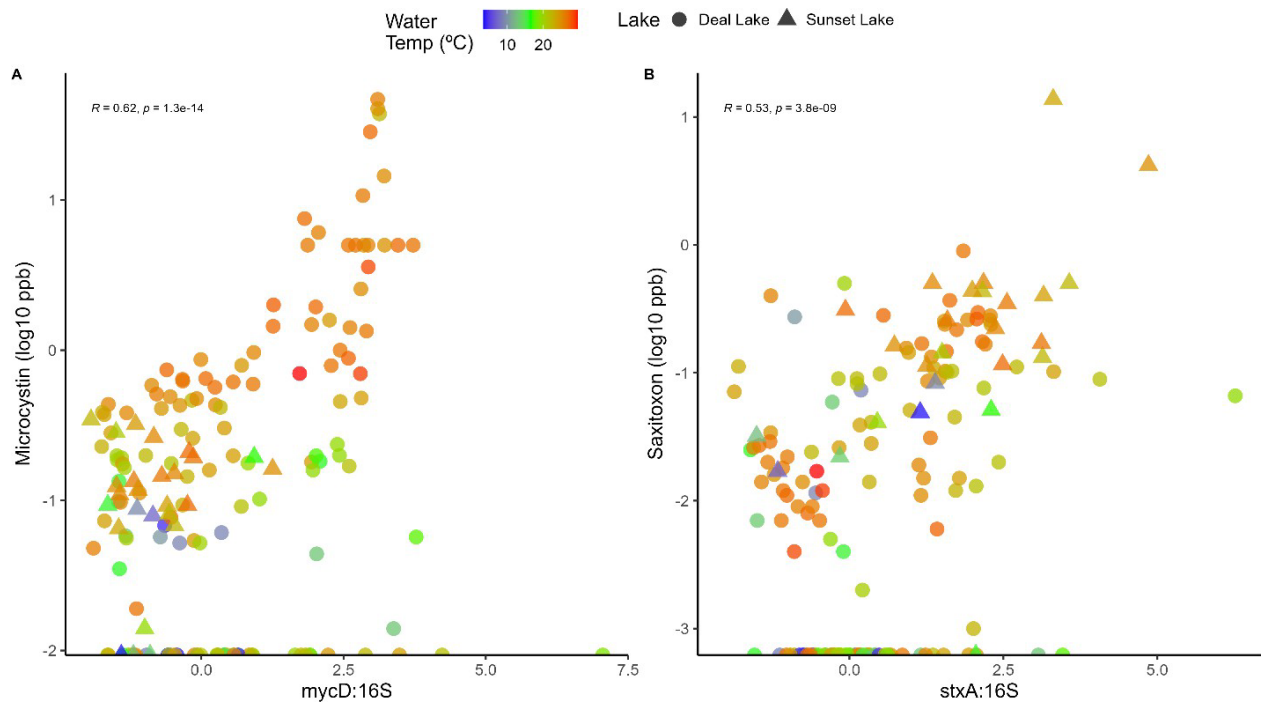


Fig. 12 Same as Fig. 11 but with toxin:16S gene ratios on x-axis

The relationship between measured toxin abundance by ELISA (ppb) and toxin gene abundance (Fig. 11) or the ratio of toxin gene to cyanobacterial 16S gene abundance (Fig. 12) showed positive and statistically significant correlations. While the *mycD* ~ microcystin relationship appeared stronger than for *sxtA* ~ saxitoxin, the latter relationship improved slightly when *sxtA*:16S was used instead of absolute gene abundance (Fig. 12B). There is a data point in Fig 11A showing high *mycD* gene abundance and low ELISA microcystin level which is anomalous.

Summary for hypothesis #3

Our analyses showed statistically-significant correlations (Pearson) between qPCR results for cyanobacterial 16S genes and biomass indices of PC fluorescence (Fig. 10A: $p < 0.001$, $R = 0.77$ for 16S ~ PC fluorescence), as well as total cyanobacterial cell counts (Fig. 10B: $p < 0.001$, $R = 0.78$ for total cyanobacterial cell counts ~ 16S). Further, in the subset of samples analyzed, a statistically significant positive correlation (Pearson) between respective ELISA toxin levels and qPCR results for microcystin (Fig 11A: $p < 0.001$, $R = 0.79$) and saxitoxin genes (Fig. 11B: $p < 0.001$, $R = 0.48$) was found as well. Relationships between gene ratios and ELISA toxin results (Fig. 12A, B) were also statistically significant but less strong than for absolute gene levels.

4. Community composition via 16S metabarcoding and relationship to cell counts

16S metabarcoding results

Metabarcoding of 16S V4 genes in Deal Lake and Sunset Lake returned 37 unique amplicon sequence variants (ASVs) from the Silva v.138.1 database (Fig. 13A). Most ASVs had genus level taxonomy in the database, and those that did not were assigned an “Unk” & the Family level taxonomy (e.g., *unk_Nostocaceae*) from the database as a name. Fig. 13A shows these ASVs as a proportion of samples in which they were detected per season for each of the lake stations samples (DL1 – DL5 and Sunset Lake). There were 16 taxa (*Cyanobium* to *Aphanizomenon* in Figure 13A) that were consistently detected across seasons and stations, except for DL5 that generally had fewer cyanobacterial detections than other Deal Lake and Sunset stations. Among these top ASVs, detections tended to be lower in spring and fall compared to summer. The ordination in Fig. 13B also reflects this, with summer (blue) samples grouping separately from spring and fall (green and red, respectively) samples. Since three dimensions were required to achieve a stress value < 0.1 (‘stress’ is an indication of how well the n-dimensional ordination reflects the underlying variability in the data. Values below 0.1 are generally considered acceptable and stress generally decreases as n-dimensions increases but interpretability becomes difficult at higher n values), the 3D stress value is shown on the plot even though only 2D are plotted. A permuted ANOVA (PERMANOVA) was run on the factor ‘season’ to determine if the seasonal grouping of points were significantly different from each other ($p < 0.05$). From this it can be concluded that cyanobacterial community composition changes by season. Some segregation of DL5 and Sunset Lake samples is also evident, particularly in summer and spring.

Fig. 14 shows the results of running a k-means (partitioning around medoids) clustering algorithm on all metabarcoding data (including cyanobacteria and all other bacteria detected). A plot similar to Fig 13 is not shown for these data because the list of all bacteria is too long to fit on a graph. The timeseries plots (Fig 14A) include the PC fluorescence (black line) showing several peaks over the year: In Deal Lake blooms are evident beginning in early July (with the exception of a small bloom in June at DL5) and through August / September. Sunset Lake shows three distinct peaks in May, July, and September. Taxonomic richness (bar height) varied among stations and over time, often showing ‘dips’ preceding and during spikes in PC fluorescence that indicated cyanobacterial blooms. The community composition of bacteria as determined by k-means clustering corresponds to the bar color, and the heatmap (Fig. 14B) shows the dominant ASVs (by relative read abundance) within each cluster. Stations DL1 – DL4 showed similar patterns of community succession leading up to the early July bloom event: Before the bloom (e.g. June) the composition was characterized by *Cyanobium* / *Pseudanabaena* cyanobacteria with *Flavobacterium* / unk_Sporichthyaceae / LD29 heterotrophic bacteria (cluster 6: dark blue / cluster 2: orange); During the bloom stations DL1 – DL4 showed to a community composition dominated by *Sphaerospermopsis* / *Pseudanabaena* cyanobacteria and LD29 heterotrophic bacteria (cluster 8: pink); after the bloom composition is more variable with DL1 and DL3 showing *Cyanobium* / *Cylindrospermopsis* / *Microcystis* / *Prochlorothrix* cyanobacteria with LD29 heterotrophic bacteria (cluster 4: green), and DL2 and DL4 showing *Cyanobium* / *Pseudanabaena* / *Sphaerospermopsis* cyanobacteria and LD29 and *Flavobacterium* heterotrophic bacteria (cluster 1: Red).

Sunset Lake composition was dominated by *Pseudanabaena* cyanobacteria and *Flavobacterium* heterotrophic bacteria (cluster : yellow) for the first bloom in May, and a mixed cyanobacterial assemblage of *Cylindrospermopsis* / *Cyanobium* / *Limnolyngbya* / *Nodosilenea* / *Sphaerospermopsis*, with *Pirellula* as the dominant heterotrophic bacterium (cluster 7: black). After October Sunset Lake bacterial community composition shifted back to what it was before the July bloom event.

It is interesting to note that, in some Deal Lake stations (DL1, DL3, and DL4) at least, the shift to the community composition that characterized the bloom occurred before the biomass increase occurred. This indicates that such shifts in community composition, detectable 1-2 weeks in advance, may hold 1-2 week ahead forecasting value for HABs. Duan et al (2022) used cyanotoxin genes and community composition data as a forecasting method for cyanotoxins in Ohio lakes, which may serve as a template for similar analyses using NJ datasets such as were produced here. It is possible to retrieve qPCR and metabarcoding results on this timescale if a system is in place.

Summary for hypothesis #4

Metabarcoding of the 16S gene in Deal and Sunset Lakes produced measures of community composition that showed anticipated seasonal changes as well as differences between lakes. Machine-learning labelling of communities via k-means clustering allowed comparisons of 16S community composition and HABs (via PC fluorescence), indicating changes in composition associated with HABs. Qualitative comparisons of 16S metabarcoding results show some

agreement and some discrepancy related to the differences in methodological biases. In particular, 16S metabarcoding detected picocyanobacterial that are not visible under the microscopic methods employed.

Environmental DNA – 16S metabarcoding

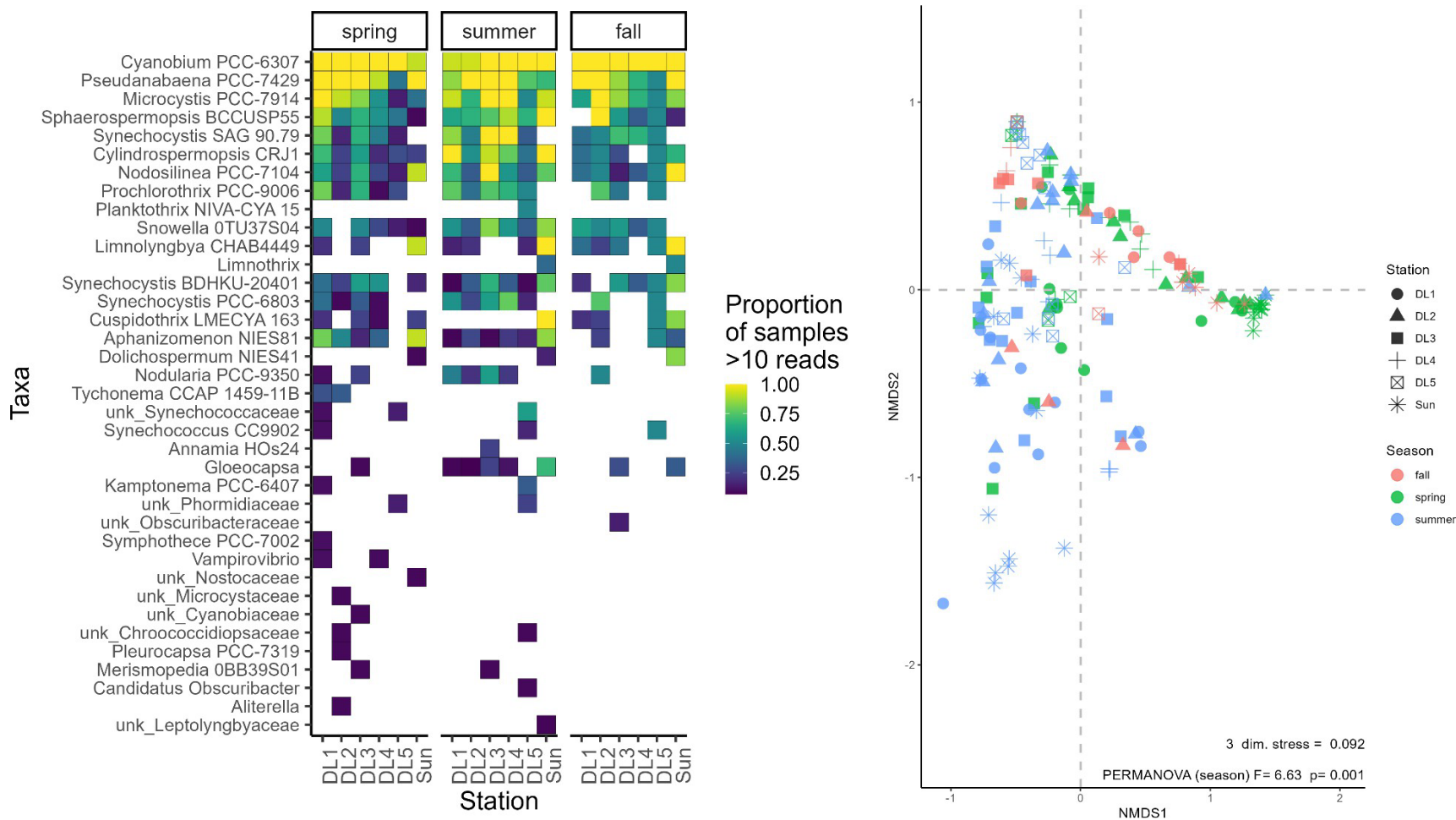


Fig 13. 16S (2021-2023) metabarcoding data (filtered to include only cyanobacteria) (A) used to identify dominant cyanobacterial taxa in the samples analyzed, (B) and perform an nMDS ordination of the samples based on the cyanobacterial community composition. In (A), more prevalent taxa are at the top of the Y axis.

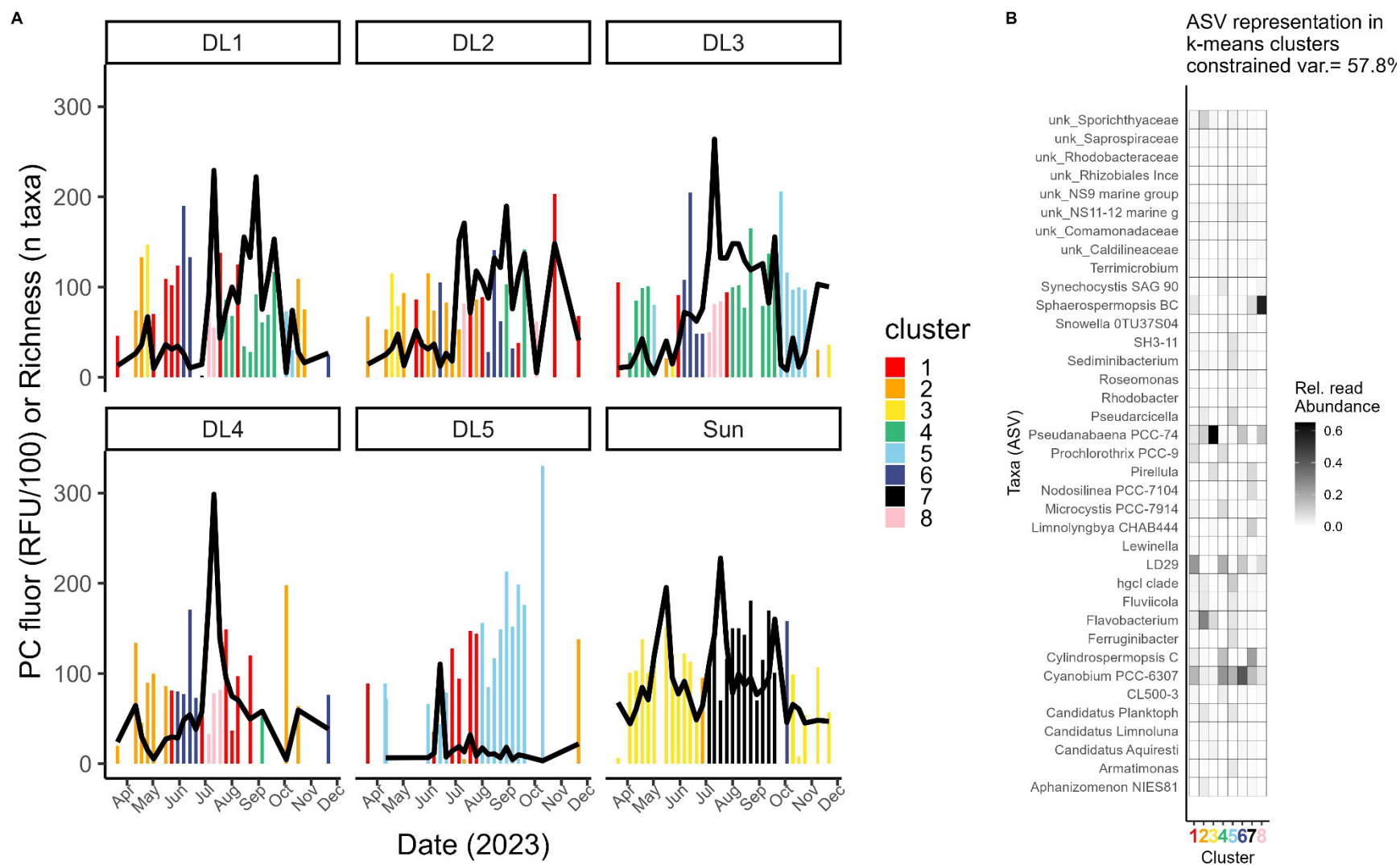


Fig. 14. Time series of bacterial community composition (for all taxa, not filtered for only cyanobacteria) as determined through k-means clustering analyses.

(A) Time series of PC fluorescence (black line), taxonomic richness (column height) and k-means community composition (column color). (B) Heat map of taxa in clusters representing community composition

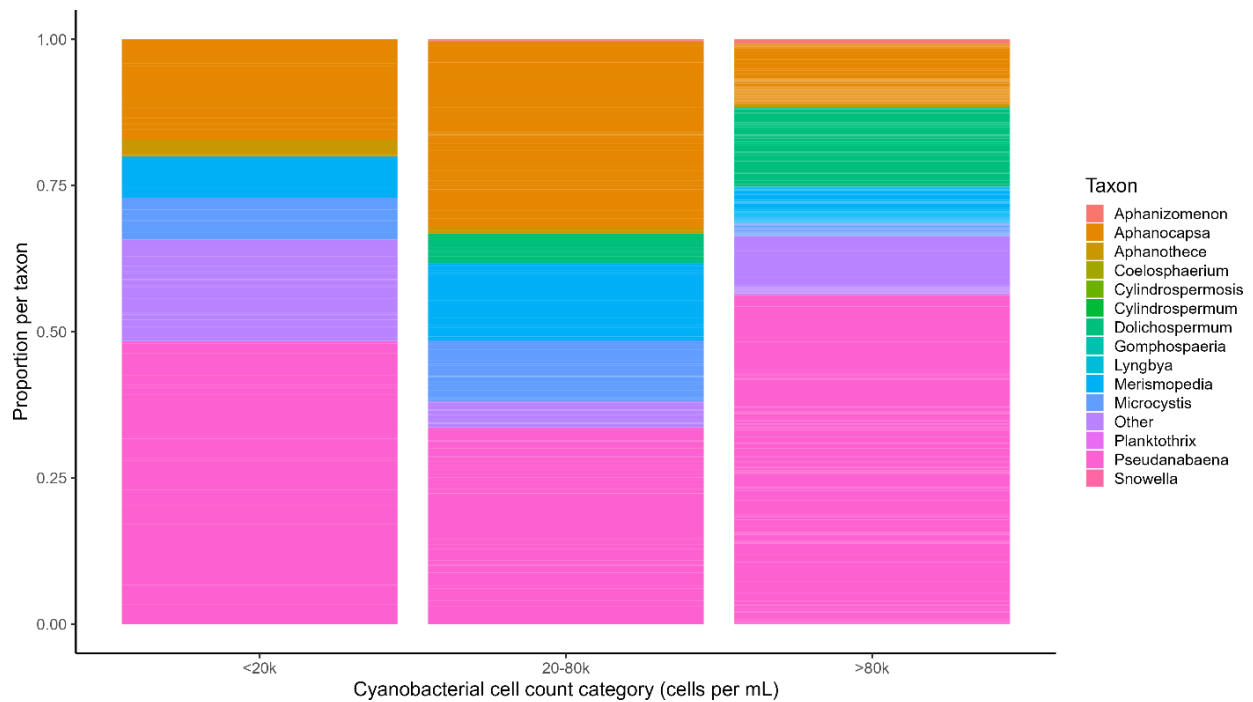


Fig 15. Proportion of taxa in cell count samples for the period May 18, 2021 – Nov 30, 2023 produced for comparison with metabarcoding results over that same time period.

5. Does rainfall predict HAB events or the expansion in Deal and Sunset Lakes?

This question is addressed by examining correlation matrices between HAB-associated parameters and rainfall measured as cumulative rainfall amounts relative to the sampling date. Correlation matrices were examined by station but there was no sub-setting by time (e.g., season). Parameters including phycocyanin fluorescence (pcrfu) and nutrients are shown across the lower axis, with cumulative rainfall on the vertical axis, summed over the indicated number of days (1d, 2d, 3d, etc...) preceding sampling. Where Pearson correlations were significant ($p < 0.05$), the color coding indicates the correlations coefficient (red = (+) correlation, blue = (-) correlation). The sampling location and sample size for that location are shown in the title of each graph. Sunset Lake 2 is excluded to save space as it looked exactly like Sunset Lake.

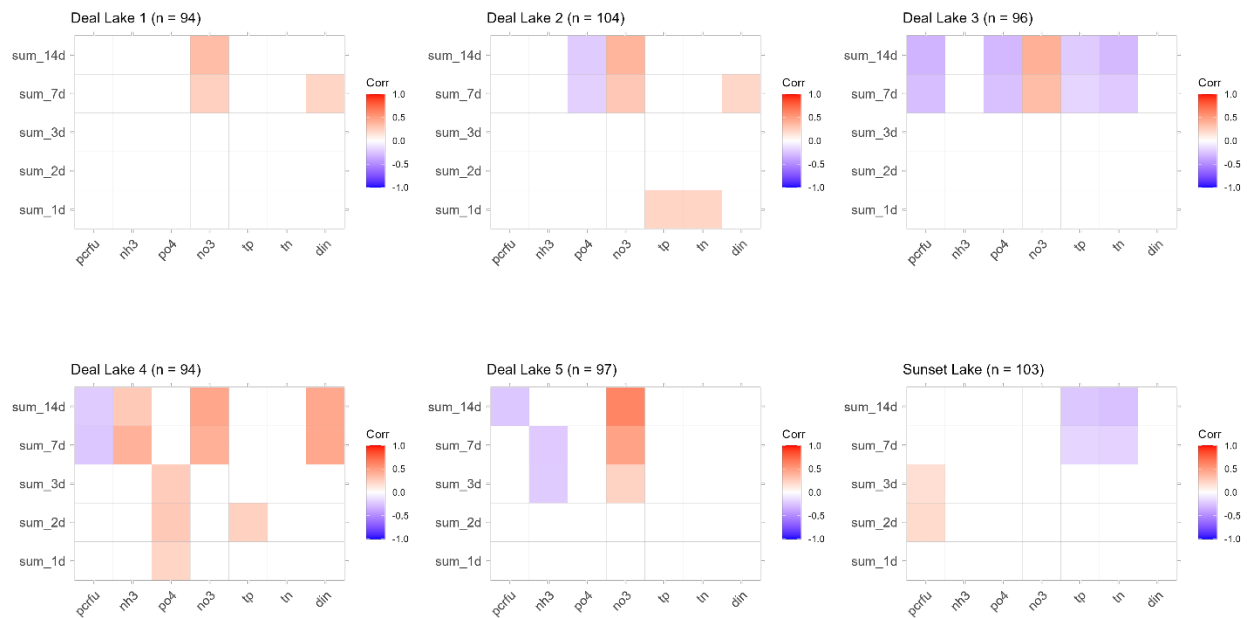


Fig. 16 Heat maps showing correlations between rainfall metrics ~ cyanobacterial biomass and nutrient parameters. Only statistically significant ($p < 0.05$) shown as colors, with red indicating positive correlations and blue negative correlations. Rainfall (y-axis) is computed as the cumulative rainfall for the n-days before sampling. Parameters (x-axis) are pcrfu = PC fluorescence (CyanoFluor), nh3 = ammonium, po4 = phosphate, no3 = nitrate + nitrite, tp = total phosphorous, tn = total nitrogen, din = dissolved inorganic nitrogen (nh3+no3).

General observations drawn from correlation heat maps in Fig. 16 include:

1. Rainfall correlations with parameters are different among DL stations.
2. In Deal Lake, NO₃ was (+) correlated to 7 d and 14 d rainfall at all stations.
3. In Deal Lake, NH₃ was (+) correlated to 7 d cumulative rainfall but only at station 4.
4. In Deal Lake, PO₄ was (+) correlated to 3 d cumulative rainfall but only at station 4.
5. In Deal Lake, phycocyanin fluorescence (pcrfu) tended to be (-) correlated with 7-14 d cumulative rainfall.
6. In Deal Lake, PO₄, TN, and TP tended to be (-) correlated with 7-14 d cumulative rainfall at stations DL1 – DL3 (lower lake (eastern basin) stations).
7. In Sunset Lake, TN and TP were (-) correlated with 7-14 d cumulative rainfall.

Summary for hypothesis #4

With regard to the original hypothesis, the negative correlation found between PC fluorescence and rainfall supports the conclusion that rain (within a week or two of sampling) tends to suppress HAB biomass in Deal Lake. This is likely caused by either a ‘washout’ effect, or by lower levels of sunlight that would be expected to be associated with rainfall. The positive correlation of NO₃ at all Deal Lake stations, as well as with NH₄ and PO₄ at DL4, supports the conclusion that rainfall can be a significant source of inorganic N to Deal Lake. Interestingly,

this was not seen for Sunset Lake, rather a (-) correlation of rainfall with both TN and TP supported a likely ‘washout’ relationship.

6. Are there relationships between water quality parameters (including HABs) and teleost fish in these coastal lakes that indicate potential impacts across trophic levels?

Environmental DNA – 12S metabarcoding (fish)

Metabarcoding analyses of fish was carried out on Deal Lake and Sunset Lake samples in order to examine potential linkages between water quality, HABs and upper trophic levels.

A total of 69 samples, spanning March – Nov 2023, eDNA extracts were analyzed for teleost fish through metabarcoding (Fig. 17). The inventory of fish in these samples (Fig. 17A) reflects taxa we expected to find in these lakes (Bluegill, White Perch, American Gizzard Shad, Common Carp, Pumpkinseeds) as predominantly detected taxa, but also other taxa that were likely present solely as genes that were advected in from adjacent ocean waters (e.g., Tautog, Broad Striped Anchovy, Atlantic Sturgeon) or through bird activity moving between the ocean and inland nests. For instance, tautog is a structure associated fish that can be found living among the groynes (locally known as ‘jetties’) on New Jersey beaches, and since the pipe connecting Deal Lake to the ocean terminates on a jetty tautog genes likely flow into Deal Lake on a regular basis and can be detected at eastern stations (DL1 and DL2). Nonetheless there is value in these data as a tool for assessing biodiversity in these habitats as has been done in other habitats (Stoeckle et al. 2020, 2022). The nMDS ordination (Fig 17B) is based on relative abundance within samples and shows a clear distinction in fish population between Sunset Lake and Deal Lake. The difference is apparent in the way a number of Sunset Lake samples cluster together in the lower right quadrant of the 2D plot, separate from other samples. Taxa driving this difference included Grass or Silver Carp, Pumpkinseed and Brown Bullhead. Interestingly, and in contrast to cyanobacterial metabarcoding results, ‘season’ did not significantly explain any of the clustering observed, consistent with their being little seasonality to fish community composition in Deal and Sunset Lakes. The greater degree of connectivity to the ocean in Deal Lake over Sunset Lake is likely a major contributor to differences in fish community composition between these two lakes.

Summary for hypothesis #5

The combination of metabarcoding datasets for both cyanobacteria and fish in the same study provides a mechanism to examine the relationship between the two communities’ dynamics. All DNA extracts used for fish metabarcoding were taken in concert with the water quality and HAB data in this study, allowing for examination of direct relationships between the two sets of data. Such relationships were examined here by testing correlations between water quality parameters, including an indicator of HAB biomass, against the relative abundance of each fish taxa’s genes. Table 3 shows the results of this analysis by indicating either a positive (+) or negative (-)

correlation between the indicated water quality or HAB parameter and the relative abundance of a taxon's genes. A negative correlation with salinity was seen for several taxa (Brown Bullhead, Catfish, Golden Shiner, Pumpkinseed), consistent with their freshwater preference. Atlantic silverside and Atlantic mackerel showed negative correlation with water temperature, but these taxa are probably not present in the lakes and what we detect is their genes which have been advected or otherwise transported to the lakes. It is unclear why these would have a negative correlation with water temperature. American gizzard shad is a common freshwater – brackish fish that showed a positive correlation with dissolved oxygen in this dataset. American gizzard shad has been observed to avoid low oxygen areas (Miller 1960) and has been described as a fish with a low tolerance of low dissolved oxygen (Williamson and Nelson 1985). On the other hand, Golden shiner, a fish that has been shown to have a high tolerance for low dissolved oxygen (<https://dep.nj.gov/njfw/wp-content/uploads/njfw/Golden-Shiner.pdf>) showed a negative correlation with dissolved oxygen in this study when the data were subsetted for Deal Lake only (not shown). Three taxa (brown bullhead, menhaden / river herring, white perch) showed a negative correlation with the HAB indicator, PC fluorescence (pcrfu). The “Atl_menhaden_LS16_or_river_herring” ASV is shared by menhaden, blueback herring, and alewife (e.g. ‘river herring’) meaning that without further investigation we cannot distinguish which fish was present. While it is unlikely that menhaden entered Deal Lake it is possible that the river herring do so as they are anadromous and Deal Lake is connected to the ocean. The decreased relative abundance of Brown bullhead and White perch may indicate sensitivity to HAB biomass leading to avoidance or mortality, consistent with negative impacts of cyanobacterial HABs on fish that have been noted in the literature (Igwaran et al. 2024). It is difficult to imagine why America eel, an anadromous fish that could conceivably enter Deal Lake through its ocean connection, would have a positive correlation with cyanobacterial HAB biomass.

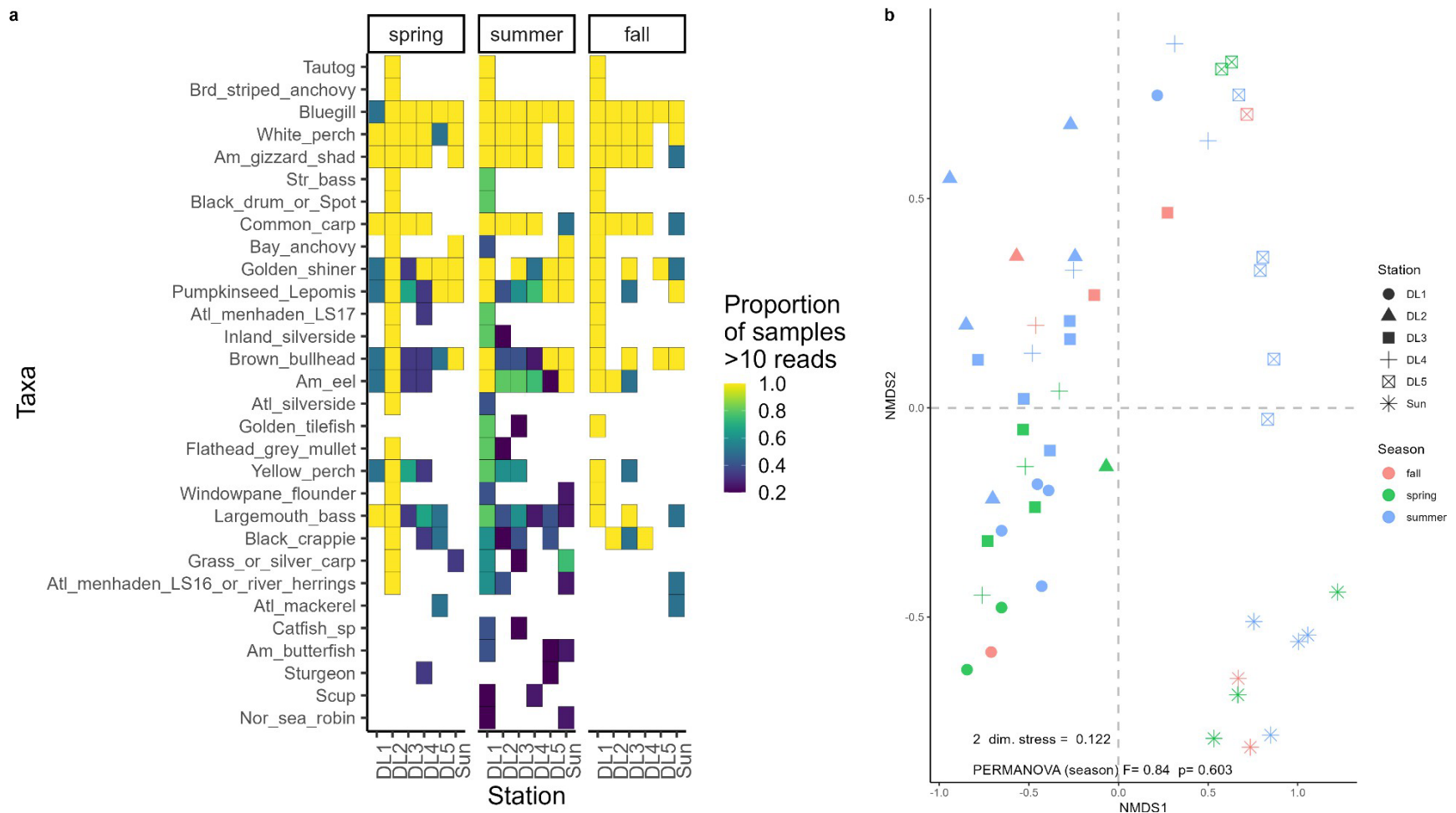


Fig. 17. eDNA 12S metabarcoding results for Deal Lake and Sunset Lake. Only results for teleost fish are included here although the reference database contains non-fish vertebrates. (A) presence of taxa expressed as the proportion of samples in which they were detected by station and season. (B) nMDS ordination to identify similar samples (using relative abundance of taxa within a sample) based on clustering in 2D space. It is important to note here that detection of fish genes can occur separate from fish presence, and with Deal Lake's connection to the ocean it is likely that some marine taxa detected are the result of advection of genes into the lake, not the organism.

Table 3: List of teleost fish taxa with a statistically significant ($p \leq 0.05$) relationship with target environmental parameters (salinity, temperature, dissolved oxygen, and PCRFU). (+) indicates a positive correlation and (-) indicates a negative correlation. Tests were conducted on combined data for Deal and Subset Lakes.

Taxon (ASV)	Salinity	Temperature	Dissolved Oxygen	PCRFU
Am_eel				+
Am_gizzard_shad			+	
Atl_mackerel		-		
Atl_menhaden_LS16_or_river_herring				-
Atl_silverside		-		
Brown_bullhead	-			
Catfish_sp	-			
Golden_shiner	-			
Pumpkinseed_Lepomis	-			
White_perch				-

Citations

- Adolf, J. E., Saldutti, K., Conlon, E., Ernst, E., Heddendorf, B., Shifren, S., & Schuster, R. (2022). *Nitrogen-limited Cyanobacterial Harmful Algal Blooms in Deal Lake, New Jersey* (Vol. 9, Issue 57). <http://www.eaglehill.us/urna>
- Callahan, B. J., McMurdie, P. J., Rosen, M. J., Han, A. W., Johnson, A. J. A., & Holmes, S. P. (2016). DADA2: High-resolution sample inference from Illumina amplicon data. *Nature Methods*, 13(7), 581–583. <https://doi.org/10.1038/nmeth.3869>
- Caporaso, J. G., Lauber, C. L., Walters, W. A., Berg-Lyons, D., Lozupone, C. A., Turnbaugh, P. J., Fierer, N., & Knight, R. (2011). Global patterns of 16S rRNA diversity at a depth of millions of sequences per sample. *Proceedings of the National Academy of Sciences of the United States of America*, 108(SUPPL. 1), 4516–4522. <https://doi.org/10.1073/pnas.1000080107>
- Duan, X., Zhang, C., Struewing, I., Li, X., Allen, J., & Lu, J. (2022). Cyanotoxin-encoding genes as powerful predictors of cyanotoxin production during harmful cyanobacterial blooms in an inland freshwater lake: Evaluating a novel early-warning system. *Science of the Total Environment*, 830. <https://doi.org/10.1016/j.scitotenv.2022.154568>
- Feng, L., Wang, Y., Hou, X., Qin, B., Kuster, T., Qu, F., Chen, N., Paerl, H. W., & Zheng, C. (2024). Harmful algal blooms in inland waters. In *Nature Reviews Earth and Environment* (Vol. 5, Issue 9, pp. 631–644). Springer Nature. <https://doi.org/10.1038/s43017-024-00578-2>
- Igwaran, A., Kayode, A. J., Moloantoa, K. M., Khetsha, Z. P., & Unuofin, J. O. (2024). Cyanobacteria Harmful Algae Blooms: Causes, Impacts, and Risk Management. In *Water, Air, and Soil Pollution* (Vol. 235, Issue 1). Institute for Ionics. <https://doi.org/10.1007/s11270-023-06782-y>
- Karosienė, J., Savadova-Ratkus, K., Toruńska-Sitarz, A., Koreivienė, J., Kasperovičienė, J., Vitonytė, I., Błaszczyk, A., & Mazur-Marzec, H. (2020). First report of saxitoxins and anatoxin-a production by cyanobacteria from Lithuanian lakes. *European Journal of Phycology*, 55(3), 327–338. <https://doi.org/10.1080/09670262.2020.1734667>
- Lopez, C. B., Jewett, E. B., Dortch, Q., Walton, B. T., & Scientific, H. K. 2008. (n.d.). Scientific Assessment of Freshwater Harmful Algal Blooms Interagency Working Group on Harmful Algal Blooms, Hypoxia, and Human Health. In *Human Health of the Joint Subcommittee on Ocean Science and Technology*.
- MacKeigan, P. W., Garner, R. E., Monchamp, M. È., Walsh, D. A., Onana, V. E., Kraemer, S. A., Pick, F. R., Beisner, B. E., Agbeti, M. D., da Costa, N. B., Shapiro, B. J., & Gregory-Eaves, I. (2022). Comparing microscopy and DNA metabarcoding techniques for identifying cyanobacteria assemblages across hundreds of lakes. *Harmful Algae*, 113. <https://doi.org/10.1016/j.hal.2022.102187>

- Miller, R. R. (1960). Systematics and Biology of the gizzard shad (*Dorosoma cepedianum*) and related fishes. U.S. Fish and Wildlife Service, *Fisheries Bulletin* 173, Vol 60
- Riaz, T., Shehzad, W., Viari, A., Pompanon, F., Taberlet, P., & Coissac, E. (2011). ecoPrimers: inference of new DNA barcode markers from whole genome sequence analysis. *Nucleic acids research*, 39(21), e145. <https://doi.org/10.1093/nar/gkr732>
- Soo, R. M., Woodcroft, B. J., Parks, D. H., Tyson, G. W., & Hugenholtz, P. (2015). Back from the dead; the curious tale of the predatory cyanobacterium *Vampirovibrio chlorellavorus*. *PeerJ*, 2015(5), 1–22. <https://doi.org/10.7717/peerj.968>
- Souza, S. (2011). The Deal Lake Watershed Protection Plan. <https://www.nj.gov/dep/wms/bears/docs/DealLakeWatershedPlan.pdf>
- Stoeckle, M. Y., Adolf, J., Charlop-powers, Z., Dunton, K. J., Hinks, G., & Vanmorter, S. M. (2020). Trawl and eDNA assessment of marine fish diversity, seasonality, and relative abundance in coastal New Jersey, USA. *ICES Journal of Marine Science*. <https://doi.org/10.1093/icesjms/fsaa225>
- Stoeckle, M. Y., Adolf, J., Ausubel, J. H., Charlop-Powers, Z., Dunton, K. J., & Hinks, G. (2022). Current laboratory protocols for detecting fish species with environmental DNA optimize sensitivity and reproducibility, especially for more abundant populations. *ICES Journal of Marine Science*, 79(2), 403–412. <https://doi.org/10.1093/icesjms/fsab273>
- Teneva, I., Mladenov, R., & Dzhambazov, B. (2009). Toxic effects of extracts from *Pseudoanabaena galeata* (Cyanoprokaryota) in mice and cell cultures in vitro. *Scientific Researches of the Union of Scientists in Bulgaria-Plovdiv, XII (Series B), XII(November)*, 237–243.
- Tiedemann, J. A., Witty, M., & Souza. (2009). *The Future of Coastal Lakes in Monmouth County*.
- Williamson, K.L. and P.C. Nelson. (1985). Habitat Suitability Index Models and Instream Flow Suitability Curves: Gizzard Shad. U.S. Fish and Wildlife Service, Fort Collins, CO.